Transport Policy 190 (2027) 104503

Contents lists available at ScienceDirect

Transport Policy

journal homepage: www.elsevier.com/locate/tranpol

From prediction to intervention: Probabilistic waiting time forecasting for resilient port management under tropical cyclones

Ruikai Sun [a], Huanhuan Li [b,*], Hao Rong [a,**], Zaili Yang [a]

[a] Liverpool Logistics, Offshore and Marine (LOOM) Research Institute, Liverpool John Moores University, Liverpool, UK
[b] School of Engineering, University of Southampton, Southampton, UK

ARTICLE INFO

Keywords:
Port resilience
Dynamic capability theory
Tropical cyclone disruption
Probabilistic forecasting
Vessel waiting time

ABSTRACT

Tropical cyclones disrupt port operations by causing temporary closures and recovery-phase vessel backlogs, which prolong waiting times and increase emissions. This study examines how probabilistic waiting time forecasts can support coordinated arrival management during post-cyclone recovery. Drawing on port resilience and dynamic capability theory, forecasting is treated as an analytical input to organisational sensing, while a conceptual mapping links its use to actors, decision points, information exchanges and actions across sensing, seizing and reconfiguring. Using a vessel-call dataset constructed from cyclone-port events across major East Asian ports from 2019 to 2025, four interpretable cyclone indicators are constructed to capture event frequency, peak intensity, duration, and cumulative exposure. Ten forecasting models are evaluated under alternative training-data and feature configurations using deterministic and probabilistic performance measures. Models trained on normal operating conditions transfer poorly to the evaluated post-cyclone contexts, whereas training on cyclone-related observations substantially improves predictive performance. Cyclone indicators provide further gains in quantile random forest (QRF) point prediction accuracy, with the selected QRF achieving an MAE of 1.808 h and an RMSE of 5.260 h. Its probabilistic forecasts are subsequently used in speed-adjustment scenario simulations for two illustrative port cases. The results show how forecast quantiles and notification lead times shape the trade-off between emissions reduction and late-arrival risk when vessels follow specified adjustment rules. The findings illustrate how probabilistic forecasts can inform recovery-stage arrival coordination by making uncertainty and operational trade-offs explicit. Dynamic capability theory provides a conceptual framework for interpreting how organisations translate forecast information into coordinated action.

1. Introduction

Climate change is increasing ports' exposure to extreme weather events, including sea-level rise, storm surges, and intensified wind systems (Stott, 2016). Among them, tropical cyclones are among the most disruptive forces on port operations, frequently triggering temporary closures and operational slowdowns. East Asia is both highly exposed to tropical cyclones and home to several of the world's busiest container ports. Consequently, cyclone-induced disruptions generate recurrent shocks to regional maritime systems and pose persistent risks to trade continuity and supply chain stability (Li et al., 2024; Liu and Chan, 2022).

Although the direct disruption during a cyclone is typically short-lived, growing empirical evidence shows that the post-cyclone recovery phase constitutes the primary source of efficiency loss. From a port resilience perspective, tropical cyclones can be viewed as acute external shocks that reduce port system functionality and trigger a recovery process (Verschuur et al., 2020). In this context, port resilience is reflected not only in whether operations resume after reopening, but also in how quickly vessel flows, berth utilisation, and service reliability return to acceptable levels. After reopening, ports often experience a backlog of vessel arrivals, leading to offshore queues and anchorage congestion (Jian et al., 2019; Lam et al., 2017). Evidence from tropical cyclone Veronica, for example, suggests that berth waiting time becomes a major contributor to total delay once operations resume (Zhang et al., 2024). Vessel waiting time, therefore, serves as a direct indicator of post-cyclone performance deterioration, reflecting both reduced service efficiency and declining schedule reliability. Managing the spillover and

* Corresponding author.
** Corresponding author.
E-mail addresses: Huanhuan.Li@soton.ac.uk (H. Li), H.Rong@ljmu.ac.uk (H. Rong).

https://doi.org/10.1016/j.tranpol.2026.104503
Received 22 May 2026; Received in revised form 21 September 2026; Accepted 21 October 2026
Available online 22 October 2026
0967-070X/© 2026 The Authors. Published by Elsevier Ltd. This is an open access article under the CC BY license (http://creativecommons.org/licenses/by/4.0/).

accumulation of waiting time during tropical cyclones has thus become a shared operational challenge for port authorities and carriers.

Although port resilience clarifies what needs to be protected and restored, it does not fully explain how uncertain disruption signals can be translated into coordinated actions and rational policy developments. Dynamic capability theory provides an advanced mechanism-oriented explanation. In turbulent environments, organisations need sensing, seizing and reconfiguring capabilities to identify change, mobilise responses and reallocate resources (Teece, 2007). The microfoundations of sensing increasingly depend on analytical systems that can extract actionable signals from complex data (Mikalef et al., 2019). In the context of tropical cyclones, sensing cannot rely only on meteorological warnings. Port authorities and terminal operators need to interpret evolving cyclone-port conditions and communicate their operational implications to carriers. Probabilistic waiting time forecasts can support this activity, providing information for joint arrival decisions and subsequent adjustments to vessel and port operational plans.

Despite growing research on maritime disruptions, quantitative analysis to support this sensing function remains limited. Most vessel delay studies focus on the estimated time of arrival during the vessel call, rather than the vessel waiting time during port congestion. Where waiting time is modelled, queuing approaches and deterministic forecasts are dominant (Jiang et al., 2024; Jo et al., 2025). However, waiting time distributions under disruptions are often highly skewed with heavy tails (Kong et al., 2022). Deterministic predictions cannot capture tail risk, dispersion in uncertainty, or asymmetric loss exposure (Huang et al., 2025). This limitation restricts the ability to define risk-sensitive operational thresholds, particularly in post-cyclone contexts characterised by rapid state transitions. Moreover, deterministic forecasts may fluctuate substantially across updates, reducing decision stability and undermining trust in predictive guidance. The lack of probabilistic forecasting thus represents, from both theoretical and practical managerial perspectives, a significant gap in how to improve sensing capability during recovery. Within this context, this study examines four research questions.

RQ1. How can a waiting time prediction model trained under normal operating conditions generalise to cyclone-disrupted contexts?
RQ2. To what extent do cyclone-port impact indicators improve predictive performance relative to models that exclude information related to disruptions?
RQ3. Which factors have the strongest influence on vessel waiting time outcomes under tropical cyclone impact?
RQ4. How can quantile-based prediction be integrated into risk-aware arrival management to support resilient post-cyclone recovery while accounting for service and environmental costs?

To address these questions, an integrated prediction to intervention framework is developed, centred on probabilistic forecasting of vessel waiting time after tropical cyclones. In the prediction stage, cyclone-port events from East Asia are first identified to construct disruption indicators, after which vessel call level observations are used to train quantile-based waiting time models. Interpretable impact indicators are designed to capture event frequency, peak intensity, duration, and cumulative exposure. These indicators are combined with vessel characteristics and port conditions to estimate the conditional distribution of waiting time, with historical waiting time information examined through comparative experiments. In the intervention stage, distributional forecasts are embedded in a speed-adjustment scenario simulation. The approach examines how part of anchorage waiting time can be shifted to controlled low-speed sailing and evaluates the associated emissions and late-arrival outcomes. Scenario simulations vary forecast quantiles and notification lead times to quantify these trade-offs and identify where additional emission benefits diminish.

This study makes three new contributions.

1) It constructs a framework from prediction to intervention for post-cyclone port recovery. Drawing on port resilience and dynamic capability theory, the study conceptualises tropical cyclones as external shocks that degrade port functionality and trigger recovery. Within this framework, probabilistic waiting time forecasting provides analytical support for sensing, while coordinated arrival decisions and implementation of agreed adjustments are interpreted as seizing and reconfiguring. A conceptual mapping links these stages to specific actors, decision points and information exchanges, clarifying the organisational conditions for applying the framework.
2) It develops an uncertainty-aware waiting time prediction model for tropical cyclone disruptions. By linking tropical cyclone characteristics with quantile modelling, the proposed approach represents variation and tail risk in waiting time outcomes. Comparisons across training settings and feature configurations, together with SHAP and indicator-level ablation analyses, assess the predictive value of cyclone information alongside vessel and port characteristics.
3) It translates probabilistic forecasts into operation management interventions. By integrating quantile waiting time forecasts with speed adjustment rules and scenario simulation, the study evaluates emissions-delay trade-offs across forecast quantiles and notification lead times in two illustrative port cases. The framework provides decision support for ports and carriers considering coordinated arrival adjustments, while identifying the participation and governance conditions required for implementation.

The remainder of the paper is organised as follows. Section 2 reviews the literature on tropical cyclone impacts on ports, vessel delay prediction, and disruption management from a dynamic capability perspective. Section 3 describes the data, event construction, impact indicators, prediction models and speed adjustment simulation. Section 4 reports predictive performance, feature comparisons and predictive contributions. Section 5 discusses the simulated intervention outcomes, the proposed coordination process and policy implications. Section 6 concludes and outlines directions for future research.

2. Literature review

This section first discusses port resilience and dynamic capability theory as complementary perspectives for understanding post-cyclone port recovery. It then summarises research on ports under tropical cyclone disruptions, focusing on how congestion and waiting times emerge. Finally, it reviews key advances in ship delay prediction, which provides the foundation for the methods and scenario analysis developed in the following sections.

2.1. Port resilience and dynamic capability under disruptions

Port resilience provides a system-level perspective for understanding how transport infrastructures withstand, adapt to, and recover from disruptive events (Mattsson and Jenelius, 2015; Wan et al., 2018). In port systems, resilience is reflected not only in whether operations can resume after a disruption, but also in how quickly service capacity, vessel flows, berth utilisation, and schedule reliability return to an acceptable level (Mohsendokht et al., 2026a; Qin et al., 2025). This recovery-oriented perspective is particularly relevant to tropical cyclone disruptions, where the direct closure period may be relatively short, but post-event vessel backlogs can continue to degrade operational efficiency after port reopening. Existing studies on port resilience under tropical cyclone hazards commonly distinguish between different temporal phases of disruption, including pre-event preparedness, disruption-period absorption, and post-event recovery (Mohsendokht et al., 2026; Verschuur et al., 2020). They also emphasise that resilience depends on multiple system capabilities, including robustness, redundancy, flexibility, rapidity, and recoverability (Bruneau et al., 2003). These concepts clarify what needs to be protected, maintained,

or restored during and after a disruption. However, they provide less direct explanations of how ports and shipping actors can translate uncertain environmental signals into timely operational decisions.

Dynamic capability theory complements this resilience perspective by explaining the organisational and analytical mechanisms through which uncertain disruption signals can be converted into coordinated action. Building on the resource-based view, Teece et al. (1997) define dynamic capabilities as the ability to integrate, build, and reconfigure internal and external competencies in response to rapid environmental change. At the capability level, Winter (2003) distinguishes ordinary or zero-order capabilities, which support routine short-term operations, from dynamic capabilities, which extend, modify, or create such routines when existing ways of working become insufficient. Teece (2007) further specifies three micro foundations of dynamic capabilities: sensing, seizing, and reconfiguring. These refer respectively to identifying opportunities and threats, mobilising resources within time-critical decision windows, and redeploying assets, processes, and organisational arrangements under changing conditions. Applied to disruption-prone port operations, this framework shifts attention from resilience as a system outcome to the processes through which actors detect risks, select responses, and adjust operational arrangements as disruptions unfold.

The link between dynamic capabilities and resilience has been increasingly recognised in crisis management and supply chain research. These studies show that resilience is not limited to recovery after a shock, but also involves preparation, response, learning, and continuous adjustment. Research integrating dynamic capability theory with disaster and crisis management suggests that threats and opportunities may activate different capabilities at different stages, thereby supporting resilience through leadership, network relationships, organisational culture, and readiness for change (Prayag et al., 2024). Related reviews in supply chain resilience similarly frame resilience as a firm-level dynamic capability, emphasising preparation, response, and recovery in the face of potential or realised disruptions, while maintaining efficiency and competitive advantage (Dovbischuk, 2022; Stadtfeld and Gruchmann, 2023). This literature suggests that effective resilience governance depends not only on the availability of resources, but also on the ability to acquire, process, and transform disruption-related information into actionable decisions.

In shipping and maritime logistics, uncertainty is increasingly frequent and compound, due to geopolitical tensions and climate-related disruptions (Liu et al., 2025). When container shipping firms face economic uncertainty and market volatility, adaptation-related dynamic capabilities become important for sustaining advantage. These capabilities are often reflected through a chain of service capability, coordination capability, and operational reconfiguration (Kuo et al., 2017). For shocks that are difficult to anticipate, such as armed conflict or route security events, firms are more likely to undertake short-term tactical redeployment rather than structural change (Yang, 2026). Improving the predictability and measurability of disruptions, therefore, strengthens the quality of sensing and expands the scope for seizing and reconfiguring. In the context of digital transformation, multiple case studies of maritime supply chains identify digital sensing, seizing, and transforming capabilities and highlight the role of visibility and transparency in resilience (Wohlleber et al., 2024). Related work on shipping firm resilience also shows that safety management practices and cross-organisational resource mobilisation can be viewed as a dynamic capability process for integrating internal and external resources (Tak et al., 2016). Consistent with broader freight resilience research, human capital and digital resources associated with Industry 4.0 can enhance resilience by improving network integration and operational planning, reinforcing the foundational role of data and analytical capabilities in building dynamic capabilities (Balci et al., 2026).

Despite these contributions, an important gap remains in how the sensing function can be effectively operationalised in acute disruption contexts. Existing maritime and supply chain studies often assess dynamic capabilities through conceptual frameworks, expert judgement, survey-based measures, case studies, or firm-level performance relationships (Bathke et al., 2024; Kuo et al., 2017; Wohlleber et al., 2024; Yang and Hsu, 2018). These approaches help explain whether sensing, seizing, and reconfiguring capabilities exist and how they relate to organisational resilience. However, they provide limited guidance on how sensing can be implemented as a quantitative, updateable, and operationally actionable tool during an unfolding disruption. Recent research on foresight and resilience in shipping emphasises the need for analytical tools that enable earlier identification of low-probability, high-impact disruptions and highlights forecasting as a mechanism for coping with technological and market change (Bathke et al., 2024). More generally, research on disaster adaptation indicates that proactive responses often depend on early warning systems and predictive monitoring that help organisations anticipate evolving disruptions and strengthen risk identification, assessment, and mitigation processes (Neise and Revilla Diez, 2019).

This gap is particularly relevant to post-cyclone port recovery. In this context, sensing cannot rely solely on meteorological warnings. Ports and carriers need to understand how cyclone-port interactions translate into actual operational outcomes, particularly vessel waiting time, because it directly reflects recovery-stage congestion and service deterioration. Without reliable probabilistic prediction tools, decision-makers may struggle to coordinate arrival management before congestion intensifies. Therefore, this study conceptualises probabilistic waiting time forecasting as an analytical tool supporting the sensing activities of port authorities and terminal operators. By converting cyclone characteristics, port conditions and vessel attributes into distributional estimates of waiting time, such forecasting provides information that these actors can interpret and share with shipping companies. Seizing occurs when ports, terminals and carriers use this information, together with berth availability and voyage constraints, to agree on feasible arrival adjustments. Reconfiguring involves implementing and updating the agreed vessel-speed and arrival plans as operational conditions change. Section 5.3 maps these stages to specific actors, decision points and information exchanges. This interpretation links predictive analytics to organisational decision-making without treating forecasting performance as a direct measure of dynamic capabilities.

2.2. *Tropical cyclone impact on maritime transportation*

One major theme in the port tropical cyclone literature is risk assessment and loss quantification, which focuses on which ports are more exposed and how large the losses may be. Studies commonly follow a hazard exposure vulnerability logic, first characterising hazards such as cyclone intensity and frequency, then combining these with measures of exposure and vulnerability, including throughput and infrastructure features, to produce risk maps and indicators. For ports in East Asia, existing work has proposed integrated approaches that combine tropical cyclone characteristics with port information to support risk assessment and adaptation planning (Jian et al., 2019; Wang et al., 2024a). More recent research has advanced integrated frameworks that couple post-event port recovery models, economic loss assessment, and shipping network resilience evaluation, arguing that recovery efficiency is a key determinant of network resilience (Wang et al., 2026). A related direction uses engineering simulation and disaster risk analysis. It estimates direct and indirect damage from tropical cyclones using terminal operation simulation, historical disaster records, and operational data, and evaluates worst-case losses under extreme scenarios (Abdelhafez et al., 2021; Cao and Lam, 2018; Lam et al., 2017). In the broader climate change context, work has also adopted multi-hazard frameworks to assess the combined impacts of sea level rise, storm surge, precipitation, wind, and heat on operational risks across global ports, providing a baseline for later high-resolution adaptation analysis (Izaguirre et al., 2021). More recently, risk

assessment studies have begun to integrate simulation-based frameworks. For example, Mohsendokht et al. (2026b) develop a hybrid probabilistic-deterministic framework for Kaohsiung Port that combines cyclone frequency-intensity modelling, asset-specific fragility analysis, and terminal operations simulation to estimate throughput loss, downtime, and direct and indirect economic losses. This line of work extends the hazard-exposure-vulnerability logic by connecting risk estimates to post-event port functionality and restoration processes.

A second theme focuses on measuring disruptions and explaining operational mechanisms after events, often using AIS and other data to reconstruct how port functions decline and how long recovery takes. Representative studies build cross-port, cross-event disruption databases and propose indicators such as total affected days and recovery capacity to characterise pre-event, during-event, and post-event dynamics. They also highlight that key assumptions used in many modelling studies still lack systematic empirical testing (Verschuur et al., 2020). In parallel, vessel-level studies explain the micro-level sources of delay during tropical cyclones. They show how rerouting, loss of control, and waiting to enter port jointly contribute to route deviation and time loss, and use Bayesian networks to link tropical cyclones, ports, and vessels for inference on delay outcomes (Zhang et al., 2024).

A third theme examines cascading effects and network-level resilience. It asks how disruptions at one or more ports propagate through shipping or port networks, resulting in system-wide efficiency losses. Such studies often use complex network methods, representing ports as nodes and routes as edges. They evaluate impacts using metrics such as network efficiency, shortest path length, and robustness. Simulation studies on regional shipping networks report that simultaneous failures at multiple ports can reduce network efficiency far more than failure at a single port, highlighting the importance of shortening recovery time for trade and supply chain stability (Huang et al., 2024; Wang et al., 2024a). Other work embeds cyclone-driven port disruptions into time-varying performance curves for global liner networks and measures resilience using the area of the curves and related metrics (Xu et al., 2024). This line extends analysis from single port loss to system-level risk, but it often relies on simplified assumptions about behavioural adjustment and recovery pathways.

Across these three themes, the most direct consequence of tropical cyclones for port systems is a decline in operational efficiency. At the micro-operational level, this deterioration often arises because port closures and traffic control measures disrupt normal arrival patterns. As vessels accumulate offshore while waiting for port entry, anchorage queues form, and congestion emerges, increasing vessel delays and system-wide operational costs (Jian et al., 2019; Lam et al., 2017; Zhang et al., 2024). Existing studies further suggest that such efficiency losses can be mitigated through improved forecasting accuracy and through coordinated operational responses, including regional traffic coordination or early speed-reduction strategies that smooth vessel arrivals (Cao and Lam, 2018; Wang et al., 2024b). From a dynamic capability perspective, such reconfiguration actions depend on timely sensing supported by actionable information. However, much of the current literature focuses on risk assessment, impact quantification, or retrospective reconstruction of disruption events. Tools that directly support operational decision-making by quantitatively predicting post-cyclone port efficiency, particularly vessel waiting time, remain limited. This gap constrains the ability of ports and carriers to anticipate congestion dynamics during recovery and to implement timely coordination measures that reduce delay accumulation.

2.3. Vessel waiting time prediction

Research on predicting vessel waiting time and port efficiency broadly follows two main streams. The first is grounded in queuing theory and berth allocation modelling. Waiting time is typically defined as the interval from arrival at the anchorage or waiting area outside the port to berthing and the start of berthing operations. Optimisation and analytical models are commonly applied to explain congestion dynamics and support berth scheduling and capacity planning (Jo et al., 2025; Yu et al., 2018; Zhang et al., 2025). However, many of these models rely on simplifying assumptions, such as stationary arrival processes, time-independent service rates, or predefined distributional forms. While such assumptions facilitate analytical tractability, they limit the ability to capture time-varying service capacity, vessel behavioural responses, and rapidly changing system states during disruption events. As a result, their applicability is constrained in highly dynamic operational environments.

The second research stream focuses on predicting arrival times, particularly the estimated time of arrival, using AIS and related data to improve berth and resource planning (Alessandrini et al., 2019; Chu et al., 2024; Saber et al., 2025; Yoon et al., 2023). These studies apply statistical and machine learning techniques to enhance arrival time prediction during vessel calls. However, AIS-based ETA values are often manually entered and subject to considerable uncertainty. Empirical evidence also indicates that ETA sequences provided by shipping lines are systematically optimistic and have limited predictive reliability (Veenstra and Harmelink, 2021). Consequently, ports frequently lack reliable, forward-looking information for operational coordination.

Because these approaches primarily support routine operations, they tend to focus on improving arrival timing or estimating average system performance rather than forecasting vessel waiting time itself. Under high-uncertainty shocks, such as tropical cyclones, such models may therefore fail to generate actionable risk signals regarding congestion. From the perspective of dynamic capability theory, effective sensing depends on analytical systems that continuously learn from data and support decision-makers in identifying, filtering, and calibrating threats and opportunities. Without quantitative tools that update during the post-event recovery period and provide probabilistic forecasts of waiting time as a direct measure of operational efficiency loss, ports and shipping actors face difficulties in interpreting evolving disruption signals. This limitation can narrow the window for timely response and weaken the capacity to coordinate vessel arrivals and reconfigure operational resources.

2.4. Research gaps

Taken together, the above review identifies three connected research gaps. First, although port resilience clarifies what should be protected, maintained and restored during disruption recovery, it offers a limited explanation of how uncertain environmental signals can be translated into timely operational decisions. Dynamic capability theory helps address this limitation by treating sensing as the foundation for subsequent seizing and reconfiguring. However, existing studies on shipping and resilience have mainly conceptualised these capabilities or assessed them retrospectively, rather than operationalising sensing through quantitative and updateable prediction tools. Second, research on tropical cyclone impacts on maritime transportation has made important progress in risk assessment, loss quantification, post-event disruption measurement, and network resilience analysis, but it still provides limited support for forward-looking operational decision-making during the recovery period, when congestion accumulates, and coordination demands are most acute. Third, existing studies on vessel waiting time and port efficiency prediction are largely designed for routine operational settings and rarely address post-disruption recovery under high uncertainty, particularly through probabilistic forecasts of vessel waiting time as a direct indicator of port efficiency. These gaps suggest the need for an integrated prediction to intervention approach that links port resilience, dynamic capability theory, and data-driven prediction of recovery stage port performance.

Therefore, this study positions probabilistic prediction of post-event vessel waiting time not simply as a forecasting exercise, but as an operational sensing mechanism that can support earlier coordination, more timely response, and more effective reconfiguration of port and

vessel operations during tropical cyclone recovery from a policy-making perspective.

3. Methodology

This study develops a prediction to intervention framework to operationalise the theoretical link between port resilience and dynamic capability in the context of post-cyclone port recovery. From a port resilience perspective, tropical cyclones are treated as external shocks that reduce port functionality and trigger a recovery process, while vessel waiting time is used as an operational indicator of recovery stage performance. From a dynamic capability perspective, probabilistic waiting time forecasting is conceptualised as an analytical sensing mechanism that transforms uncertain cyclone-port signals into risk information, which can then support seizing and reconfiguration through speed-adjustment decisions. The framework therefore connects disruption measurement, probabilistic prediction, risk interpretation, and operational intervention within a unified methodological structure. The framework consists of five main stages, as shown in Fig. 1.

First, AIS and vessel technical data are integrated to reconstruct vessel activity trajectories. Data cleaning and trajectory segmentation are performed to identify individual vessel call legs and extract key operational outcomes, including vessel waiting time.

Second, tropical cyclone-port events are used as the contextual framework for defining disruption phases and constructing cyclone impact indicators, while individual vessel calls constitute the modelling observations. For each cyclone event, the set of potentially affected ports is identified, and the disruption status of each port is determined. Based on these events, interpretable tropical cyclone characteristics are constructed to characterise hazard intensity and disruption exposure. Given that the candidate variables include multiple vessel, port, tropical cyclone and historical features, the Least Absolute Shrinkage and Selection Operator (LASSO) is applied as a feature selection method to reduce dimensionality, mitigate multicollinearity and construct a parsimonious modelling dataset (Muthukrishnan and Rohini, 2016; Tibshirani, 1996).

Third, the vessel-call dataset is partitioned into training, test and simulation sets using cyclone-port events as the grouping unit. Two events are reserved for simulation. Five-fold event-grouped cross-validation is conducted within the training set to select feature-screening settings and model hyperparameters. Fitted preprocessing steps, including standardisation and LASSO screening, use only the corresponding training folds and are subsequently applied to the validation folds. The selected configurations are then refitted on the full training set and evaluated on the held-out test set.

Fourth, to improve interpretability and clarify the driving mechanisms of congestion, Shapley Additive Explanations (SHAP) are employed to identify the most influential factors affecting waiting time outcomes during disruption periods (Xu et al., 2026). This step is included because predictive accuracy alone cannot explain why congestion risk increases or which operational factors drive post-cyclone recovery outcomes. SHAP provides a transparent basis for linking model predictions to congestion mechanisms and for supporting the subsequent intervention analysis.

Finally, the selected predictive model is embedded within a speed-adjustment strategy designed to mitigate congestion and reduce emissions. A scenario-based simulation is used to evaluate the intervention's performance across different forecast quantiles and notification lead times. These two dimensions represent, respectively, the degree of risk conservatism embedded in decision-making and the timeliness of information available for operational coordination. The associated sensitivity analysis serves two purposes for validation. It tests the robustness of the estimated balance between emission reduction and delay under alternative decision settings, and examines whether the proposed forecasting to intervention mechanism produces stable and interpretable operational responses under different uncertainty and timing conditions.

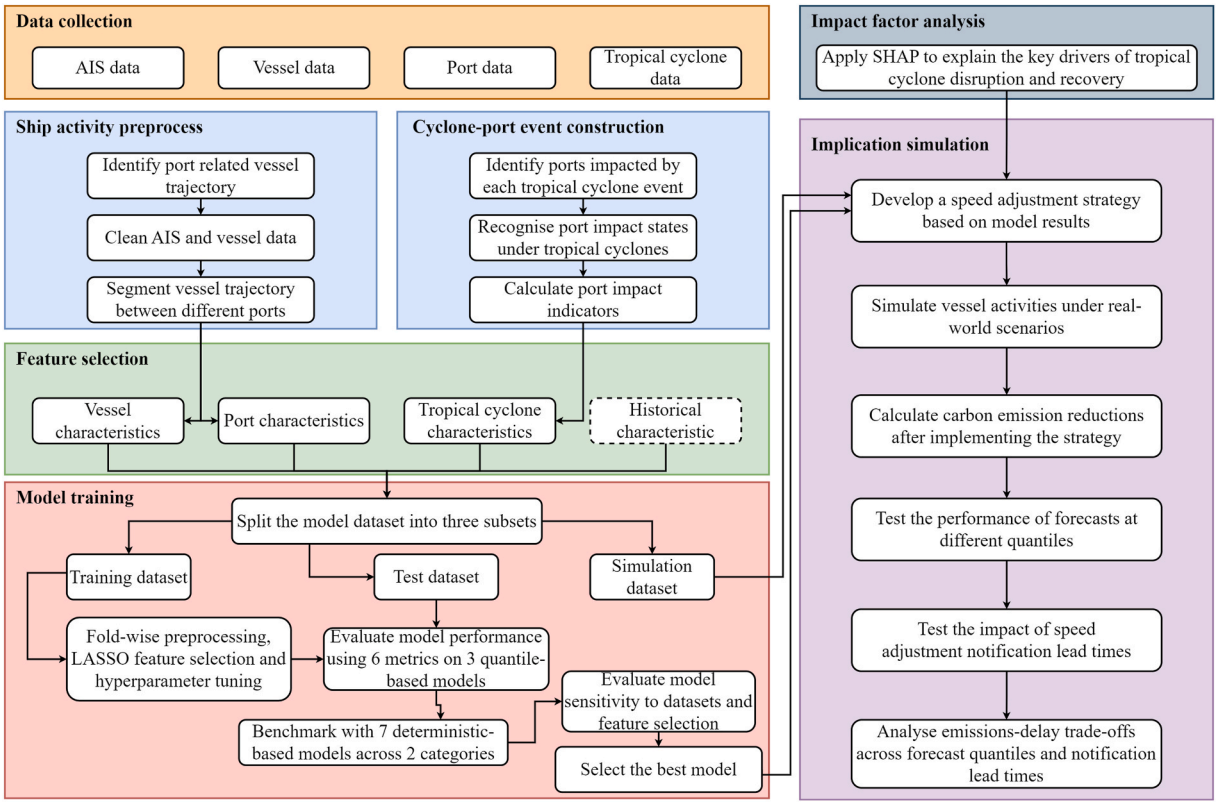

Fig. 1. Research framework of this study.

3.1. Cyclone-port event construction

The empirical analysis focuses on East Asia, a region characterised by dense port networks and intensive maritime traffic (Noorali et al., 2022), while also representing one of the most active areas globally for tropical cyclone occurrence. The study period covers 2019 to 2025, reflecting the timeframe for which consistent data are available. Consistent with previous AIS-based research examining port activity before, during and after natural disasters (Verschuur et al., 2020), this study adopts an observation window extending from 30 days before each tropical cyclone starts to 60 days after it ends. The pre-event period provides observations for establishing baseline port activity, while the post-event period allows delayed congestion and subsequent recovery to be observed. This common window supports consistent comparisons across cyclone-port events.

Tropical cyclone events are identified using the PortWatch platform, which provides information on cyclone tracks and associated maritime impacts. Study ports are selected based on annual vessel traffic thresholds to ensure sufficient operational activity for meaningful analysis. Specifically, ports handling fewer than 1000 vessels per year are excluded. At such traffic levels, the average daily throughput is approximately three vessels, making it difficult to distinguish cyclone-induced disruptions from normal fluctuations in port activity driven by trade variability and operational factors (Verschuur et al., 2020).

After linking tropical cyclones to ports, port states are identified using four-hourly changes in the Relative Vessel Proportion (RVP). As defined in Eq. (1), RVP is the ratio of the vessel count in the most recent 24-h window, denoted by n_t, with a baseline level, denoted by n_{base}. n_{base} is the average daily vessel count over the four weeks preceding the port's cyclone impact. Normal activity therefore corresponds to an RVP of 1.0. A 20 per cent deviation from the baseline classifies the port as abnormal (Chen et al., 2023). If RVP falls below 0.8 during the cyclone activity window, the port is classified as being in a disruption phase. If RVP later exceeds 1.2, the port is in a congestion phase. Tropical cyclone impacts on port operations are typically short, lasting only a few days (Verschuur et al., 2020). Therefore, if congestion does not occur within one week after the end of the disruptions, the event is treated as having no congestion effect.

$$\mathrm{RVP}_t = \frac{n_t}{n_{base}} \tag{1}$$

Building on this, four port level impact indicators are used to describe tropical cyclone effects at the port level, as illustrated in Fig. 2. Tropical Cyclone Frequency (TCF) measures the cumulative number of tropical cyclones recorded as affecting a port from the start of 2019 up to the occurrence time of the focal cyclone-port event. Cyclones occurring after the focal event are not included. Tropical Cyclone Peak Intensity (TCPI) reflects the severity of an event and is measured using the gap between benchmark number and minimum number of vessels in port during the impact period. Tropical Cyclone Duration (TCD) represents the duration of impact, measured from the time the cyclone begins affecting the port until vessel counts recover to at least 80 per cent of the baseline. Tropical Cyclone Cumulative Impact (TCI) measures the accumulated disruptions by integrating the gap between the observed in-port vessel count and its baseline level over the impact period. Together, these indicators quantify shocks at the tropical cyclone event and port level and provide interpretable explanatory variables for the prediction models.

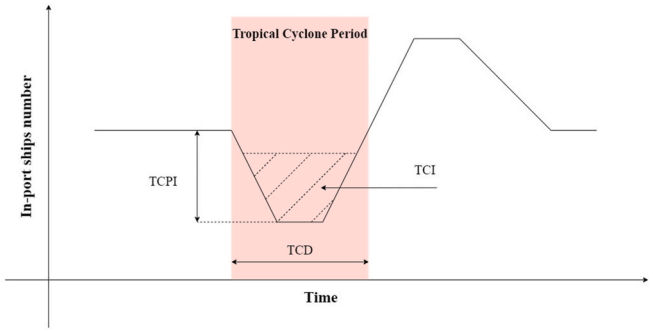

Fig. 2. Port impact indicators under tropical cyclones.

3.2. Ship activity preprocess

AIS records for vessels calling are first extracted at ports that are affected by tropical cyclones during the study period. Container shipping exhibits relatively regular calling patterns and is often more sensitive to delays, so this research focuses on container vessels. The AIS trajectories are cleaned by removing abnormal points via consistency checks between the coordinate-based average speed and the reported AIS speed. Records are classified as abnormal when the recorded speed exceeds 30 knots or is below 0 knots. Missing records are filled using linear interpolation (Yan et al., 2025). Interpolation is restricted to gaps of 24 h or less and longer gaps are left not interpolated. Trajectory segmentation is applied to split vessel movements into port legs. A standard leg is defined from the time a vessel leaves the previous port area to the time it leaves the area of the current calling port. Port entry and exit are identified using an 80-nautical-mile radius around the port reference point, which encompasses the anchorage areas of most ports (Liu et al., 2026). This produces standardised vessel call units that support the calculation of waiting time and emissions. Finally, vessel activity states are identified using vessel speed, engine power, and distance to port. These states include sailing, manoeuvring, berthing, and anchoring. The classification thresholds for each state are reported in Table 1, according to IMO report (IMO, 2020a). Vessel waiting time is calculated as the sum of the durations of all anchoring episodes within each vessel call. Calls with missing activity timestamps or incomplete trajectories that prevent the calculation of waiting time are excluded. A total of 75,395 container vessel calls were identified in the cleaned AIS activity data, of which 40,584 fell within the cyclone-event study windows and filtering for positive berthing and sailing durations. For the predictor variables, port characteristics contain no missing values, whereas missing values in vessel characteristics are imputed using the method described in our previous study (Sun et al., 2025a).

3.3. Feature selection

After preprocessing, a modelling dataset is constructed comprising four groups of candidate features, as summarised in Table 2, based on previous research (Choi and Yoon, 2025; Saber et al., 2025). Vessel features capture vessel size and technical characteristics, including deadweight tonnage, draft, length overall, beam, year built, service speed, main engine rpm, and main engine power. These variables are obtained from the LSEG database. Port features describe port capacity and structure. Variables such as GDP per capita, city population, and facility capacity are collected from official city statistics and port reports. Additional port activity indicators are derived from AIS data,

Table 1
Operational phase assignment decision matrix.

SOG (knots)	ME load	Port distance ≤ 1 nm	Coast distance < 5 nm	Coast distance ≥ 5 nm
≤ 1	-	At berth	At Anchor	At Anchor
> 1 to ≤ 3	-	At Anchor	At Anchor	At Anchor
> 3 to ≤ 5	≤ 0.65	Manoeuvring	Manoeuvring	Manoeuvring
> 3 to ≤ 5	> 0.65	Manoeuvring	Manoeuvring	Cruising
> 5	-	Manoeuvring	Cruising	Cruising

Table 2
Summary of features.

Category	Feature	Description
Identification Information	IMO	Unique ship identification number
Vessel characteristics	DWT	Maximum cargo carrying capacity
	DRA	Vertical distance between waterline and keel
	LOA	Total length of the vessel
	BEAM	Width of the vessel
	Built	Year the vessel was constructed.
	SSP	Service speed of the vessel
	MER	Revolutions per minute of the main engine
	MEP	Power output of the main engine
Port characteristics	BulkP	Share of bulk vessels in total port calls
	ContP	Share of container vessels in total port calls
	GDPP	Gross domestic product per capita of the port's hinterland
	CityP	Population of a port city
	FCAP	Capacity of port infrastructure including anchorages and berths
	ANDWT	Total deadweight tonnage of vessels calling at the port annually
	PDWT	Percentage of total deadweight tonnage of daily vessels calling at the port compared with the benchmark period
	PNUM	Percentage of the total number of daily vessels calling at the port compare with the benchmark period
	MAXD	Maximum available water depth at port berths or channels
Tropical cyclone characteristics	TCF	Cumulative number of tropical cyclones affecting the port from the start of 2019 up to the occurrence time of the event.
	TCPI	Peak intensity of tropical cyclones impacting the port area
	TCD	Length of time a tropical cyclone influences port operation
	TCI	Cumulative impact of tropical cyclones on ports
Historical characteristic	BWT	Waiting time of historically similar vessels
Target characteristic	WT	Vessel waiting time at anchorage

including bulk share, container share, annual port deadweight tonnage, daily deadweight tonnage share, daily vessel share, and maximum water depth. For model training, the daily deadweight tonnage share and daily vessel share are measured one day prior to each vessel call's estimated time of arrival, while sensitivity analysis further examines alternative notification lead times from one to seven days before prediction. Tropical cyclone features include TCF, TCPI, TCD, and TCI, with definitions and calculations provided in Section 3.1. It should be noted that, in the present study, these tropical cyclone characteristics indicators are treated as inputs for recovery-stage waiting time forecasting. Specifically, the proposed model is applied once the port has entered the post-cyclone recovery or congestion phase, when disruption-related information can be identified from observed port-state changes. Although these indicators could themselves be forecast in a more anticipatory framework (Wang et al., 2020), that upstream prediction problem is beyond the scope of this study.

Historical baseline waiting time (BWT) is constructed for the comparison experiments after the cyclone-port event-level data partitioning described in Section 3.4. A k-nearest neighbours approach identifies the ten most similar eligible historical vessel calls using the vessel and port characteristics listed in Table 2 (Tak et al., 2016). BWT is calculated as the unweighted arithmetic mean of the observed waiting times of these matched calls. The reference pool is restricted to eligible historical records from the relevant training partition. A historical call is eligible only if its AIS activity sequence was completed strictly before the prediction timestamp of the target call. Calls associated with the same tropical cyclone event and any records representing the same physical vessel call as the target are excluded. For each target vessel call, duplicate records of the same historical call are counted only once in the reference pool. The same historical call may be used for multiple target calls, provided that it meets the eligibility criteria at each prediction timestamp. Simultaneous or overlapping calls that remain ongoing at the prediction timestamp are therefore excluded. Closely spaced calls are eligible only when their activities have already been completed and they satisfy the same partition, event and call-level exclusion rules. Before nearest-neighbour matching, the vessel and port characteristics are standardised using Z-scores, with means and standard deviations estimated exclusively from the eligible reference pool. The same transformation is applied to the target call and the candidate historical calls. BWT construction is repeated within the model validation procedure, using the fold-specific reference pools described in Section 3.4.

3.4. Model training

The modelling dataset is split into three subsets. These are the training, test, and simulation sets. The simulation set consists of Ningbo-Zhoushan Port under Tropical Cyclone Lekima in 2019 and Kaohsiung Port under Tropical Cyclone Haikui in 2023. Both ports have sufficient average daily vessel calls. Kaohsiung is highly exposed to tropical cyclones, whereas Ningbo-Zhoushan is less exposed, allowing the simulation to cover contrasting contexts and improving the representativeness of the results. The remaining cyclone-port events are randomly allocated to training and test sets, with all vessel calls belonging to the same event assigned to the same partition.

Model development combines preprocessing, LASSO feature screening (Muthukrishnan and Rohini, 2016) and hyperparameter tuning using five-fold event-grouped cross-validation within the training set. All calls belonging to the same cyclone-port event remain in the same fold. In each split, standardisation and LASSO screening are fitted on four folds and applied to the remaining validation fold. The LASSO penalty and model hyperparameters are selected based on cross-validation performance. Each selected configuration is then refitted on the full training set and evaluated on the held-out test set.

For configurations including BWT, matching is repeated within each cross-validation split. Fitting observations receive out-of-fold BWT values using eligible records within that split's training portion, while validation observations use eligible records from the training portion only. For final fitting, training BWT is generated out-of-fold, whereas test BWT uses eligible records from the full training set. Test and simulation records never enter reference pools, and records of the same physical call remain in the same partition and fold. The prediction time, exclusion and standardisation rules in Section 3.3 apply throughout.

The model design contains two distinct groups. The first group comprises seven deterministic based benchmark models used to compare conventional predictive performance. These benchmark models were selected according to three principles: methodological representativeness, suitability for the prediction task, and comparability under the available data conditions. Specifically, they cover the main families of deterministic models commonly used in waiting time and port performance prediction, including statistical models, tree-based machine-learning models, and other flexible nonlinear learners. The second group comprises three quantile-based models. These are not treated as benchmark models in the strict sense but are evaluated separately because the central objective of the study is to quantify predictive uncertainty and support risk-aware operational intervention. This distinction allows the analysis to compare standard deterministic prediction performance with that of distributional modelling to assess whether distributional modelling provides additional value for disruption management.

The deterministic-based benchmark models include two statistical models and five machine-learning models. The statistical models are linear regression (LR) and elastic net regression (ENR), the latter being

suited to settings with correlated predictors (Chambers and Hastie, 1992). The machine learning models are random forest (RF), bagged classification and regression trees (Bagged CART), extreme gradient boosting (XGBoost), k-nearest neighbours (KNN), and support vector machines (SVM) (Gong et al., 2025; Zhou, 2021). To quantify predictive uncertainty more directly, three quantile-based models are further evaluated: quantile linear regression (QLR), QRF, and quantile gradient boosting machine (QGBM) (Arora et al., 2023; Kang and Hansen, 2021).

Evaluation is conducted on the test set using two groups of six complementary metrics which have been widely used in the relevant literature (Hall, 1992; Hersbach, 2000; Uyanık et al., 2020). The first group widely measures deterministic prediction accuracy, capturing how closely single-valued predictions match observed waiting times (Uyanık et al., 2020), as shown in Eqs. (2)–(4). Mean absolute error (MAE) provides an intuitive measure based on the average absolute deviation. Root mean square error (RMSE) penalises larger errors more strongly through squared deviations and reflects predictive stability. R^2 evaluates the extent to which the model explains variation in the target variable. Together, these three metrics provide the baseline assessment of predictive accuracy. In Eqs. (2)–(4), y_i is the actual value, $\hat{y}_i$ is the predicted value, n is the number of examples.

$$\mathrm{MAE} = \frac{1}{n}\sum_{i=1}^{n}|y_i - \hat{y}_i| \tag{2}$$

$$\mathrm{RMSE} = \sqrt{\frac{1}{n}\sum_{i=1}^{n}(y_i - \hat{y}_i)^2} \tag{3}$$

$$R^2 = 1 - \frac{\sum(y_i - \hat{y}_i)^2}{\sum(y_i - \bar{y}_i)^2} \tag{4}$$

The second group comprises distributional accuracy metrics, which are commonly used to assess how well models quantify uncertainty (Hall, 1992; Hersbach, 2000), as shown in Eqs. (5)–(7). Coverage measures how often the observed value falls within the predicted interval and is central for checking the reliability of probabilistic intervals. Interval width reflects the sharpness of the prediction. For a given level of coverage, narrower intervals provide more informative guidance. The Continuous Ranked Probability Score (CRPS) assesses the overall quality of the predictive distribution by measuring the distance between the predicted and observed cumulative distribution functions. Compared with point accuracy metrics, these measures provide a more direct view of model reliability under strong variability. Based on their combined performance across these metrics, the best overall model is selected for the subsequent scenario simulation and strategy design. In Eq. (7), $F_i(z)$ denotes the predictive cumulative distribution for observation i. $\mathbb{I}(\cdot)$ is an indicator function, whose function is to determine the value of 1 or 0 based on whether the condition within the parentheses is true or false. Waiting time predictions, MAE, RMSE, interval width and CRPS are reported in hours.

$$\mathrm{Coverage} = \frac{1}{n}\sum_{i=1}^{n}\mathbb{I}\left(\hat{y}_i^L \le y_i \le \hat{y}_i^U\right) \tag{5}$$

$$\mathrm{IW} = \frac{1}{n}\sum_{i=1}^{n}\left(\hat{y}_i^U - \hat{y}_i^L\right) \tag{6}$$

$$\mathrm{CRPS} = \frac{1}{n}\sum_{i=1}^{n}\int_{-\infty}^{\infty}\left(F_i(z) - \mathbb{I}(z \ge y_i)\right)^2 dz \tag{7}$$

3.5. Translating forecasts into intervention

The preceding sections establish the predictive validity of the proposed framework and identify the main drivers of post-cyclone waiting time. However, predictive performance alone does not show how such information can support operational decision-making. To address RQ4, this section embeds the selected probabilistic waiting time forecast into a risk-aware intervention framework. The purpose is to examine how uncertainty-aware congestion prediction can be translated into practical arrival-management strategies that mitigate post-cyclone congestion and reduce greenhouse gas (GHG) emissions during the recovery period.

After the quantile-based waiting time prediction is obtained, speed adjustment is adopted as the core intervention for three reasons. First, it exploits the nonlinear relationship between vessel speed and energy use, allowing part of the delay that would otherwise be absorbed through anchorage idling to be reallocated to controlled low-speed sailing before arrival. Second, it is a comparatively low-cost and operationally implementable measure, as it does not require additional hardware investment and can be applied within existing vessel call planning and port coordination practices. Third, it provides a practical mechanism for balancing emissions savings against late-arrival risk under uncertain post-cyclone congestion conditions. By varying forecast quantiles within a prescribed adjustment rule, the framework compares emissions and late-arrival outcomes under alternative waiting time assumptions, without modelling how individual operators select among these scenarios.

3.5.1. Emission accounting for intervention evaluation

To evaluate the operational consequences of speed adjustment, vessel emissions are estimated using the International Maritime Organization (IMO) bottom-up activity-based approach (IMO, 2020b). The unit of analysis is a single vessel call, and the model combines high-resolution activity data with detailed vessel technical parameters to simulate energy use across operating phases. This accounting module links the simulated activity profile of each vessel call to GHG emissions, thereby providing the basis for evaluating the intervention's environmental performance. The full formulation is given in Eqs. (8)–(10).

Total emissions, denoted as $E_{t,p}$, are calculated by aggregating multiple GHG across operating phases and converting them into CO_2 equivalent using global warming potential weights GWP. Let S denote the set of operating states, including normal sailing, reduced speed sailing, anchorage waiting, and at-berth operations. Using CO_2 as an example, for each phase i, the model accounts for main engine, auxiliary engine, and boiler contributions by combining rated power P, specific fuel consumption SFC, load factors LF_{ME}, and fuel emission factors EF_{Fuel}. Phase duration is computed from distance travelled D_i and average speed $V_{i,avg}$. The main engine load factor is adjusted dynamically with speed, using the average speed $V_{i,avg}$ and the service speed $V_{service}$. This formulation captures the nonlinear effect of speed reduction on engine load and the resulting fuel use and emissions.

$$E_{t,p} = \sum_{i\in S}\left(E_{i,CO_2} + GWP_{N_2O}\times E_{i,N_2O} + GWP_{CH_4}\times E_{i,CH_4}\right) \tag{8}$$

$$E_{i,CO_2} = \left(P_{ME}\times SFC_{ME}\times LF_{ME} + P_{i,AE}\times SFC_{AE} + P_{i,BO}\times SFC_{BO}\right)\times EF_{Fuel} \times \frac{D_i}{V_{i,avg}} \tag{9}$$

$$LF_{ME} = \left(\frac{V_{i,avg}}{V_{service}}\right)^3 \tag{10}$$

3.5.2. Scenario simulation of decision performance

To evaluate the decision value of probabilistic waiting time forecasts, a scenario-based simulation model is developed. The simulation examines how quantile-based predictions translate into speed-adjustment decisions under different levels of risk conservatism and information timeliness. By utilising the potential waiting time of ships sailing at slow speeds, pressure on port resources can be alleviated (Nguyen et al., 2026). Specifically, the selected forecast quantile represents the degree of conservatism with respect to anticipated waiting time embedded

Table 3
Summary of selected cyclone-port events.

Tropical Cyclone	Year	Ports
LEKIMA-19	2019	Fuzhou, Taipei, Ningbo-Zhoushan
LINGLING-19	2019	Gunsan, Daesan, Pyongtaek
HAISHEN-20	2020	Kiire, Busan, Kwangyang, Hiroshima, Donghae, Kagoshima, Ube, Hakata, Kanda, Daesan, Gunsan, Pyongtaek, Tsukumi
CHANTHU-21	2021	Taipei, Keelung, Hualien
DOKSURI-23	2023	Quanzhou, Kaohsiung, Xiamen, Meizhou, Fuzhou
SAOLA-23	2023	Guangzhou, Huizhou, Shekou, Yantian
HAIKUI-23	2023	Kaohsiung, Xiamen, Mailiao
KOINU-23	2023	Hualien, Mailiao, Kaohsiung, Hong Kong
GAEMI-24	2024	Meizhou, Hualien, Keelung, Mailiao, Fuzhou, Quanzhou
YAGI-24	2024	Yangpu, Qinzhou, Fangcheng, Zhanjiang, Haiphong
KONG-REY-24	2024	Haimen, Hualien, Taichung, Meizhou, Fuzhou, Xiamen, Ningbo-Zhoushan, Keelung

in the prescribed speed-adjustment rule, rather than the behavioural risk preference of an individual operator. Higher quantiles use longer waiting time allowances and can permit greater speed reductions, subject to operational constraints, but may increase late-arrival exposure. The analysis therefore compares alternative adjustment settings without modelling operators' willingness to trade off anchorage waiting, schedule reliability, fuel savings and contractual penalties. The workflow is summarised in Algorithm 1.

The model starts by specifying input variables and expanding scenarios. Inputs include actual berth time T_{berth}, actual anchor waiting time T_{anchor}, berth plan notification time point t, actual sail time T_{sail}, sail distance D_{sail}. It also includes the predicted vessel waiting time at the quantile p, denoted as $T_{anchor,p}$. The algorithm iterates t from 1 to 168 h to represent different notification lead times and to generate decision scenarios under varying levels of advance information. It then simulates speed decisions based on the forecast. In each run, the available time for speed adjustment, denoted as T_{opt}, is computed using Eq. (11).

$$T_{opt} = \begin{cases} T_{sail} & , T_{sail} + T_{anchor,p} \le t \\ t - T_{anchor,p} & , T_{anchor,p} \le t \le T_{sail} + T_{anchor,p} \\ 0 & , t \le T_{anchor,p} \ or \ t = 0 \end{cases} \tag{11}$$

Combining T_{opt} with $T_{anchor,p}$ yields a theoretical reduced speed, denoted as V'_{redu}. To ensure navigation feasibility, the theoretical speed is adjusted using a minimum operation speed V_{min}, producing the simulated reduced speed V_{redu}. Based on V_{redu}, the algorithm updates the main engine load factor and recalculates the adjusted sailing duration within the speed adjustment window, yielding LF'_{ME} and T'_{opt}. Finally, the algorithm performs time reallocation and emission accounting using the simulated parameters. The difference between the T'_{sail} and T_{sail} is calculated as ΔT. This difference is used to adjust the actual vessel waiting time, producing a simulated vessel waiting time T'_{anchor} and any resulting late arrival time T_{late}, as shown in Eq. (13). Late arrival is evaluated relative to the original sailing duration plus the observed anchorage waiting time. This provides a retrospective reference rather than a confirmed berth window or actual berth availability. The updated activity profile is then passed to the bottom-up activity-based emission model to compute total GHG emissions, denoted as $E_{t,p}$ for each scenario. These outputs provide the basis for comparing the trade-off between emissions reduction and delay across different forecast quantiles and notification lead times.

$$\Delta T = T'_{sail} - T_{sail} \tag{12}$$

$$\begin{aligned} T'_{anchor} &= \max\,(0, T_{anchor} - \Delta T) \\ T_{late} &= \max\,(0, \Delta T - T_{anchor}) \end{aligned} \tag{13}$$

Algorithm 1. Speed adjustment scenario sensitivity analysis

Input: Actual berth time T_{berth}; Actual anchor waiting time T_{anchor} ; Predict anchor waiting time $T_{anchor,p}$ (at percentiles p); Berth plan notification time point t; Actual sail time T_{sail}; Sail distance D_{sail}; Minimum operation speed V_{min}; Main engine load factor LF_{ME}
Output: Total GHG emissions $E_{t,p}$ (at time point t and percentiles p); Late arrival time T_{late}
For $t = 1, \ldots, 168$ **do**
Calculate the speed adjustment time T_{opt} according to Eq. (11);
Obtain theoretical reduced speed $V'_{redu} = \frac{V_{avg} \times T_{opt}}{T_{opt} + T_{anchor,p}}$;
Update V'_{redu} using V_{min} to obtained simulated reduced speed V_{redu};
Get updated speed adjustment time T'_{opt} and updated main engine load factor LF'_{ME} based on V_{redu};
Generate simulated sail time T'_{sail};
Calculate waiting time gaps ΔT between T'_{sail} and T_{sail} according to Eq. (12);
Generate simulated anchor waiting time T'_{anchor} and T_{late} according to Eq. (13);
Input T_{berth}, T'_{sail}, T'_{anchor}, T'_{opt} and LF'_{ME} to bottom-up activity-based method to calculate $E_{t,p}$;
End
Plot sensitivity figure

4. Experimental results and analysis

This section summarises the cyclone-port event contexts used to define disruption indicators. It then presents the vessel call level training-validation-test workflow for waiting time prediction. The performance of the 10 methods is compared on the test set and concluded by examining the factors that drive waiting time prediction.

4.1. Cyclone-port event summary

Based on the collected data, 122 cyclone port events are initially identified. Among these,46 events are excluded because the associated ports record fewer than 1000 vessel calls annually, resulting in insufficient traffic levels for meaningful congestion analysis. An additional 19 events show no observable congestion following the cyclone. The remaining 57 events form the study sample, and the selected cyclone-port events are listed in Table 3. To assess the sensitivity of the findings to event selection, an expanded sample analysis incorporating the excluded events is presented in Appendix A.

To illustrate the dynamic impact of tropical cyclones on port activity, Fig. 3 presents two representative cases: Ningbo-Zhoushan Port (Fig. 3a) and Kaohsiung Port (Fig. 3b). Fig. 3 plots hourly fluctuations in RVP, aligned with the tropical cyclone timeline, where Day 0 denotes the event reference point. The black line represents the observed RVP series at four-hourly intervals, while the blue line shows a 24-h moving average that smooths short-term fluctuations and highlights the overall pattern.

In both ports, the disruptions follow a broadly similar sequence of four phases: a stable pre-event period, a sharp decline during disruption, a rapid post-cyclone surge, and a gradual recovery. Before landfall, RVP stays close to the baseline level of 1.0 in both ports, indicating normal operational conditions. As the tropical cyclone approaches, as shown by the red-shaded disruption window in Fig. 3, port closure measures and precautionary behaviour lead to a sharp decline in vessel arrivals. RVP reaches its lowest point between Day 0 and Day 2, dropping to around 0.5 of normal activity levels.

Following the storm, delayed vessels begin arriving in a concentrated manner during the congestion window highlighted in blue. RVP rises above the baseline level and produces compensatory congestion, with peak values reaching around 1.4 in both ports. Despite experiencing a similar initial disruption, the subsequent recovery patterns differ across the two cases. Ningbo-Zhoushan Port exhibits a single peak V-shaped

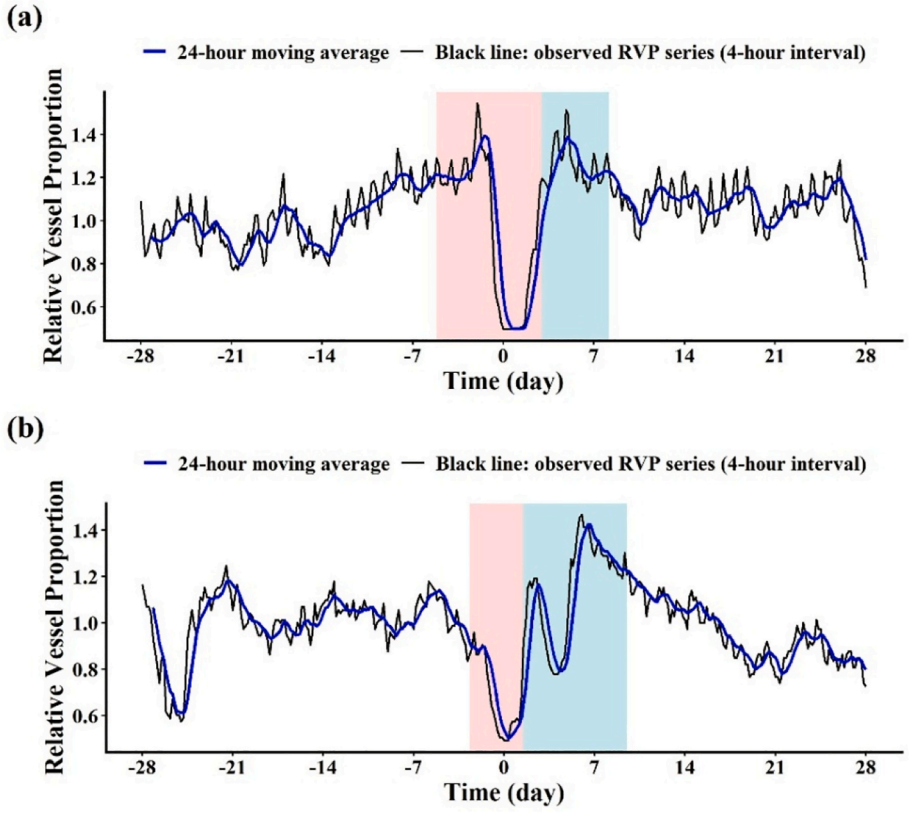

Fig. 3. Relative vessel proportion change by hour (a: Ningbo and Zhoushan; b: Kaohsiung).

rebound, suggesting a relatively rapid recovery, whereas Kaohsiung Port shows a more prolonged adjustment process with a less concentrated peak. These patterns indicate that tropical cyclones not only disrupt port capacity during the event itself but can also trigger significant downstream congestion during the recovery phase. The comparison further highlights heterogeneity in how different ports absorb disruption shocks and restore operational stability. This four-stage pattern also provides empirical support for treating cyclone disruption as a recovery process rather than as a single event. The main operational challenge does not only arise during the disruption itself, but also during the recovery stage, when the arrival of compensatory vessel calls can intensify congestion.

4.2. Experiment setting

Before model evaluation, the cleaned vessel call dataset is split in a structured manner to support both predictive benchmarking and downstream scenario simulation. First, two representative cyclone-port cases are held out as an independent simulation dataset: Ningbo-Zhoushan Port under Tropical Cyclone Lekima in 2019 and Kaohsiung Port under Tropical Cyclone Haikui in 2023. These cases are selected because both ports have sufficient daily vessel calls and represent different levels of exposure to tropical cyclones. This allows the subsequent simulation to examine the intervention framework under contrasting operational contexts. After reserving these two simulation cases, the remaining cyclone-port events are allocated to training and test partitions following Section 3.4. All vessel calls associated with an event remain in the same partition. Within these partitions, observations are classified into benchmark and post-cyclone congestion subsets. The post-cyclone observations in the test partition form the common test set for comparing the modelling settings.

Based on these data partitions, the experiments are organised in two stages. First, benchmark-period and post-cyclone training data are compared using the same port and vessel predictors. Second, within the post-cyclone setting, four feature configurations are evaluated by adding tropical cyclone indicators and BWT separately and jointly. Together, these form five modelling configurations. All configurations use the same five-fold event-grouped cross-validation procedure and common held-out test set. The retained predictors and LASSO coefficients are reported in Appendix B.

This design allows the analysis to distinguish between two research questions: whether models trained under normal or benchmark operating conditions can generalise to post-cyclone congestion contexts, and whether adding tropical cyclone information improves predictive performance once the training data already reflect disruption conditions.

4.3. Model performance

Fig. 4 compares the performance of the 10 models across two training settings, Benchmark and TC data, using MAE, R^2, and RMSE. Under the benchmark setting, predictive performance is generally weak, and R^2 is low across models. Training on cyclone-related congestion data substantially improves the performance of QRF, RF and XGBoost, whereas improvements for the other models are more limited. For QRF, MAE decreases from 11.995 to 1.889 h and RMSE from 17.448 to 5.493 h, representing reductions of 84.3% and 68.5%, respectively. R^2 increases from −0.200 to 0.881. These results indicate that training on observations representative of disrupted conditions is important for predicting post-cyclone waiting times.

Fig. 5 further examines the incremental predictive contributions of cyclone indicators and BWT under four feature configurations. Vessel and port characteristics are retained across these configurations, while cyclone indicators and BWT are included separately or jointly. QRF remains the best-performing model across all four configurations. Adding cyclone indicators without BWT reduces QRF's MAE from 1.889 to 1.808 h and RMSE from 5.493 to 5.260 h, improvements of 4.3% and 4.2%, respectively, while R^2 increases from 0.881 to 0.891. Adding BWT

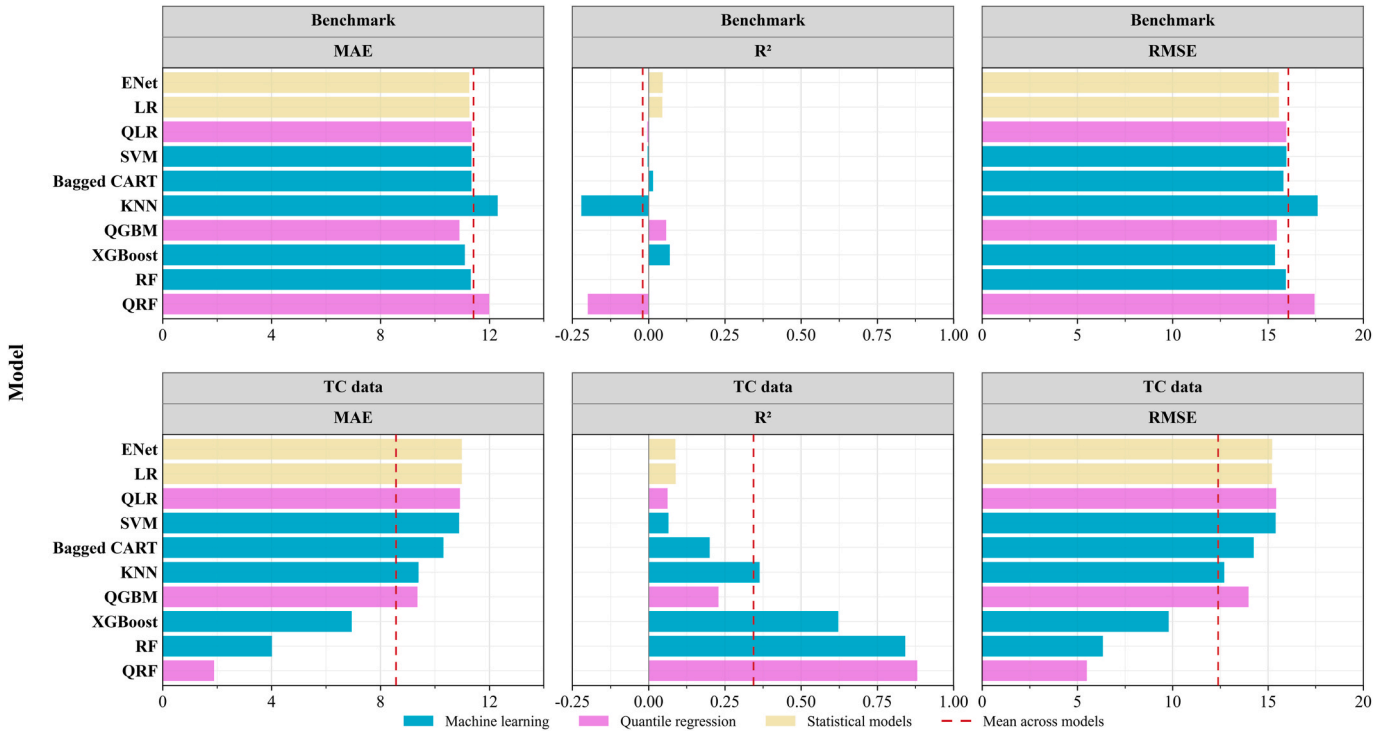

Fig. 4. Model performance by different datasets.

without cyclone indicators yields an MAE of 2.119 h and an RMSE of 5.544 h. Including both BWT and cyclone indicators yields an MAE of 2.091 h, an RMSE of 5.487 h and an R^2 of 0.881. Thus, BWT does not provide further improvements in QRF's point prediction performance. These results support using vessel, port and cyclone characteristics without BWT for the subsequent analysis. Comparing model categories, QRF and RF perform particularly well on the cyclone-related data, followed by XGBoost. The results therefore favour tree-based models.

Table 4 reports the performance of the quantile models in quantifying uncertainty under the three settings. Under the benchmark setting, the quantile gradient boosting machine achieves the lowest CRPS, while the quantile random forest provides the narrowest interval but lower coverage than the other two models. Under the TC data setting, QRF's coverage increases from 0.707 to 0.951, its interval width decreases from 24.774 to 18.490 h, and its CRPS decreases from 8.711 to 1.828 h. Adding cyclone indicators produces a smaller further change, with coverage reaching 0.954, interval width decreasing to 18.417 h, and CRPS decreasing to 1.820 h. QRF thus combines the narrowest intervals and lowest CRPS among the three quantile models under both cyclone-data settings. Coverage should be assessed against the nominal interval level, rather than interpreted as better simply because it is higher. Together with the point prediction results, these findings support selecting QRF for the subsequent speed-adjustment scenario simulation.

To illustrate the value of quantile models in managing post-cyclone uncertainty, Fig. 6 shows the predicted cumulative distribution functions for four sample vessel calls drawn from the test set, Ship #6, Ship #126, Ship #338, and Ship #788, together with their categorical probabilities. Moving from a single deterministic forecast to a distributional forecast is practically important for post-cyclone congestion management because it allows decisions to be linked to risk levels rather than a single expected value. In the figure, the black step curve represents the predicted cumulative distribution, and the blue marker indicates the observed waiting time. The background shading and the bar chart in the lower right align with three waiting time categories. These are up to 6 h as short waiting, more than 6 and up to 24 h as moderate delay, and more than 24 h as severe delay.

The results illustrate how QRF differentiates waiting time risk across these selected vessel calls. For Ship #6 and Ship #338, the model assigns the highest probability to short waiting, at 73.6 per cent and 52.5 per cent, respectively. Their observed waiting times, 5.2 h and 0.37 h, both fall within this category. However, Ship #338 also has a 40.1 per cent probability of moderate delay, indicating uncertainty across the two categories. For Ship #126, the model assigns a 60.2 per cent probability to moderate delay, and the observed waiting time of 16.31 h aligns with this prediction. Ship #788 represents a more extreme case. The model assigns a 76.1 per cent probability to waiting beyond 24 h, and the observed waiting time reaches 33.6 h. These examples illustrate how distributional forecasts communicate both likely waiting time categories and the possibility of longer delays, providing information for the subsequent speed adjustment scenario simulation.

4.4. *Impact factor analysis*

To improve transparency and examine the predictors of post-cyclone waiting time, SHAP is used to analyse feature contributions across the selected QRF model. SHAP is grounded in cooperative game theory and quantifies each feature's marginal contribution to a prediction, allowing both global and local contributions to be assessed. Fig. 7 reports global feature importance based on mean absolute SHAP values. Fig. 8 presents a bee swarm plot showing how low and high feature values relate to increases or decreases in predicted waiting time. SHAP values are expressed in hours and describe predictive contributions rather than causal effects.

The global ranking in Fig. 7 shows that BulkP is the most influential factor, followed by PDWT, FCAP and PNUM, with mean absolute SHAP values of 2.271, 1.597, 1.482 and 1.353, respectively. This pattern indicates that port traffic composition, short-term demand pressure and facility capacity provide important information for predicting prolonged waiting times during post-cyclone recovery. In contrast, vessel-specific characteristics such as deadweight tonnage, year built, and draft provide useful information. However, the highest-ranked predictors are port-level characteristics, highlighting the importance of operational

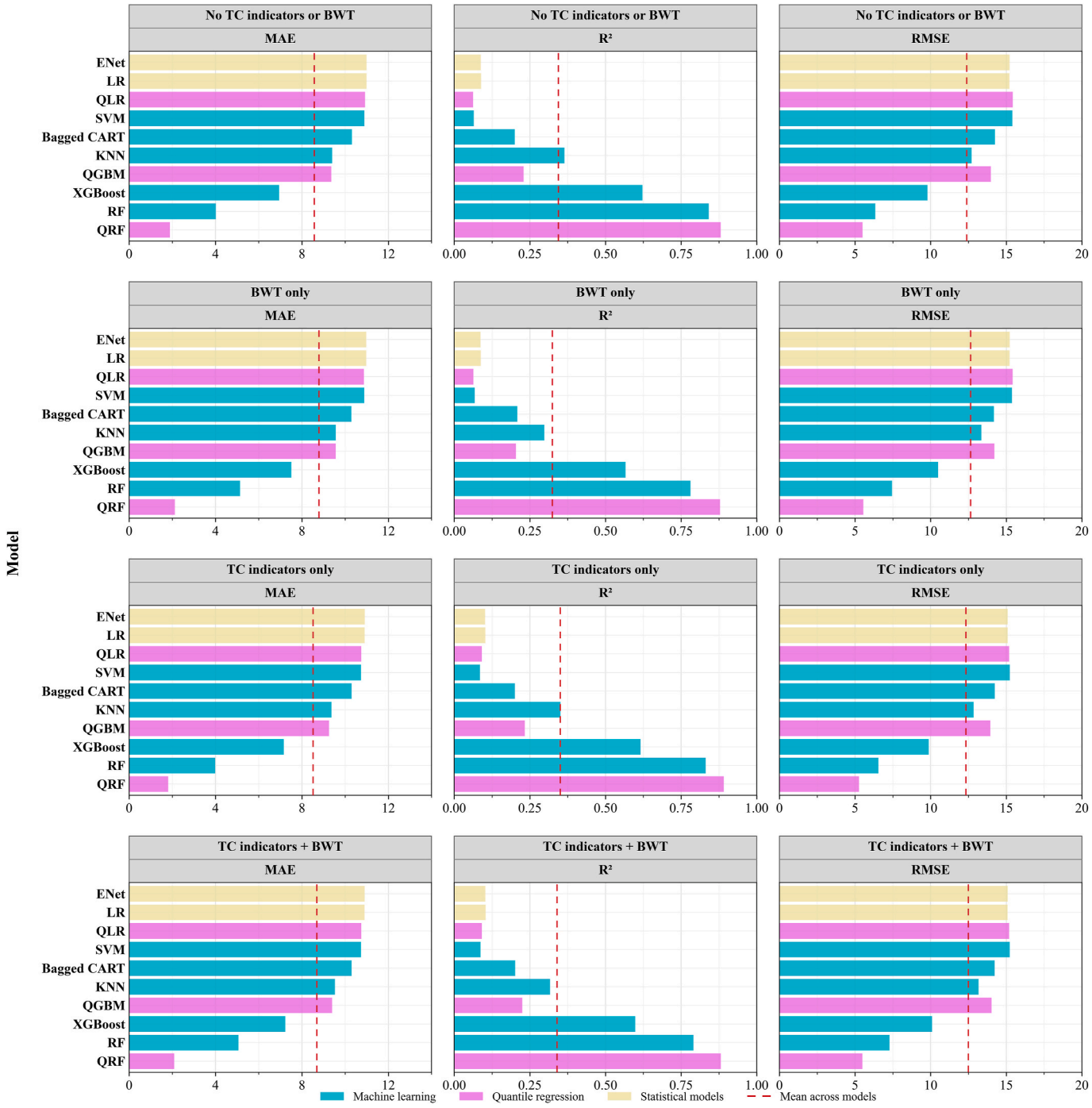

Fig. 5. Model performance by different features.

Table 4
Model performance of quantile models.

Scenario	Model	Coverage	Interval Width	CRPS
Benchmark	QLR	0.810	33.778	7.912
	QGBM	0.789	29.249	7.786
	QRF	0.707	24.774	8.711
TC data	QLR	0.825	35.271	7.624
	QGBM	0.800	30.294	6.434
	QRF	0.951	18.490	1.828
TC data + TC indicators	QLR	0.832	35.213	7.552
	QGBM	0.808	30.176	6.390
	QRF	0.954	18.417	1.820

conditions in waiting time prediction. All four cyclone indicators are retained, with TCD and TCI contributing more strongly on average than TCPI and TCF.

The bee swarm plot in Fig. 8 further clarifies the patterns of these predictive contributions. PNUM and PDWT exhibit substantial positive SHAP tails, consistent with the relevance of short-term port demand conditions to elevated waiting time predictions. However, the mixture of feature values indicates that these relationships are not uniformly monotonic. The cumulative cyclone impact indicator, denoted as TCI in the figure, also shows positive SHAP contributions for some higher values, suggesting that cumulative disruption information helps identify vessels with longer predicted waiting times. These results highlight the predictive relevance of port operating conditions and cyclone impacts,

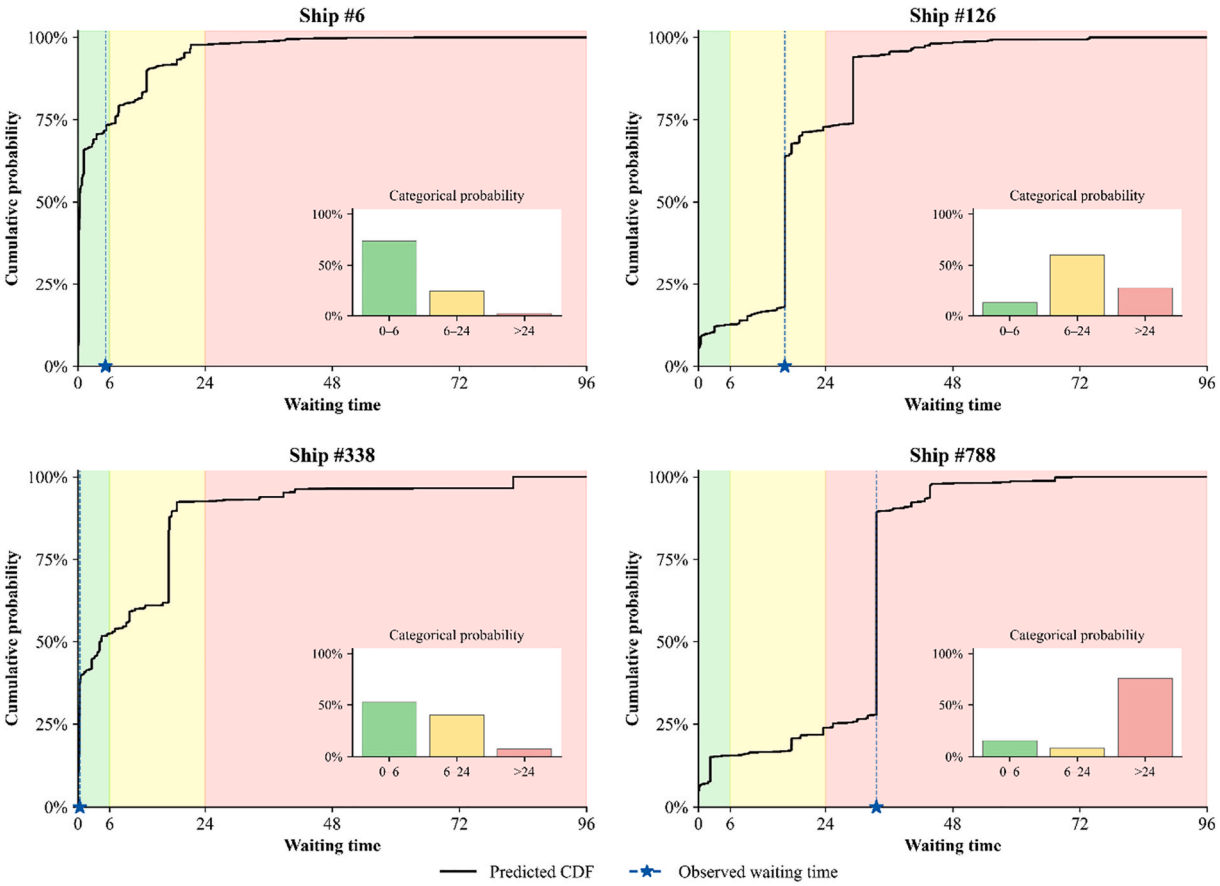

Fig. 6. Predictive cumulative distribution of different example vessel call.

without establishing independent causal effects or delay propagation.

Fig. 9 further examines the contribution of cyclone indicators through four ablation experiments, each removing one indicator while retaining the same observations, remaining predictors and QRF settings. With all four indicators, QRF achieves an MAE of 1.808 h, an RMSE of 5.260 h and an R^2 of 0.891. Removing TCF increases MAE and RMSE to 1.875 and 5.473 h, respectively, while removing TCPI increases them to 1.872 and 5.496 h. Removing TCD produces a smaller deterioration, with an MAE of 1.827 h and an RMSE of 5.309 h. Removing TCI produces the largest increase in MAE, to 1.907 h, with an RMSE of 5.486 h. These results support the incremental contribution of all four cyclone indicators to point prediction accuracy. Their value is therefore not fully reflected by their individual SHAP rankings.

5. Discussion and implications

This section discusses how the empirical findings support the proposed prediction to intervention framework for post-cyclone port recovery. It interprets probabilistic waiting time prediction as an analytical tool supporting the sensing activities of port authorities and terminal operators. The section then examines how this information can support joint arrival decisions by ports and carriers and the implementation of agreed speed adjustments. The discussion focuses on three issues, namely the value of probabilistic sensing under disruption, the translation of predictive uncertainty into risk-informed operational choices, and the policy implications for port resilience.

5.1. Disruption sensing and waiting time risk interpretation

The model results show that post-cyclone port recovery cannot be adequately modelled as a normal operating state. Models trained under normal operating conditions perform poorly when applied to tropical cyclone disruption scenarios. This finding suggests that tropical cyclones create a temporary but different operating environment, in which vessel arrival patterns, port handling capacity and congestion dynamics deviate from normal conditions. The comparison shows that training on cyclone-related observations substantially improves the performance of QRF and RF, while adding cyclone indicators provides a smaller further improvement for QRF. The improvement achieved after adding tropical cyclone characteristics further demonstrates the value of sensing disruption information. Indicators such as TCF, TCPI, TCD and TCI translate tropical cyclone characteristics into measurable operational signals. These indicators and the resulting waiting time distributions provide analytical inputs for sensing. Port authorities and terminal operators can interpret these forecasts alongside observed port conditions to identify vessel calls that may require arrival coordination. The predictive results demonstrate the informational value of these inputs.

The strong performance of the quantile random forest model also indicates that probabilistic prediction is more suitable than deterministic prediction during post-cyclone recovery. Waiting time outcomes under disruption are often asymmetric and may include high-risk tail events. A single expected value cannot show whether a vessel faces low, moderate or high congestion risk. By contrast, distributional prediction provides information on the possible range of waiting times and the probability of extreme delays. This is essential for operational sensing, as it enables ports and carriers to make decisions with clearer risk information.

The SHAP results further identify the main contributors to predicted waiting time. BulkP, PDWT, FCAP and PNUM have the highest mean absolute SHAP values, highlighting the predictive relevance of port traffic composition, short-term demand and facility characteristics. Vessel characteristics and cyclone indicators also have contributions.

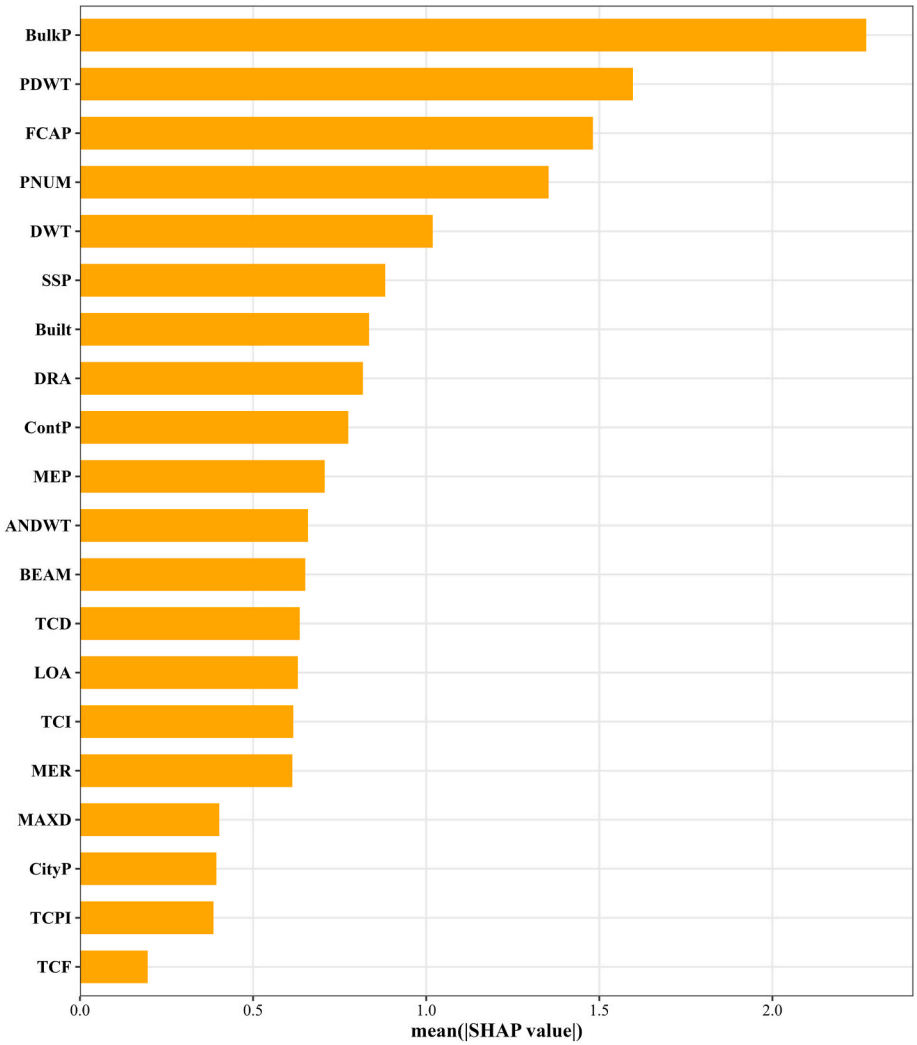

Fig. 7. Feature importance value.

Nevertheless, removing any one of these indicators increases QRF's MAE and RMSE, supporting their value for point prediction. These findings show that probabilistic forecasting can provide interpretable information on how port conditions, vessel characteristics and cyclone indicators contribute to waiting time predictions.

5.2. *Resilient port call arrival reconfiguration through speed adjustment*

To assess how probabilistic forecasts can support port-call arrival adjustment during post-cyclone recovery, Fig. 10 presents response surfaces for Ningbo-Zhoushan Port and Kaohsiung Port across different forecast quantiles and notification lead times. The analysis evaluates simulated emissions and late-arrival outcomes associated with reallocating part of the observed anchorage waiting time to controlled low-speed sailing. Forecast quantiles define alternative waiting time allowances within the prescribed adjustment rule, rather than different behavioural risk preferences. Notification lead times determine the time window available for speed adjustment before vessels reach the port area.

The heatmaps quantify the waiting shift mechanism during post-cyclone recovery. In both ports, dynamic speed adjustment before arrival shifts part of the anchorage queue into controlled low-speed sailing along the inbound leg. As indicated by the transition towards darker green areas in the heatmaps, total GHG emissions along the arrival leg decrease across much of the scenario range. The strategy changes where part of the waiting time is absorbed and reduces emissions through the associated adjustment in sailing speed and anchorage duration. This redistribution could reduce the concentration of vessels waiting near the port, although changes in port-wide queues and recovery duration are not directly evaluated in the simulation.

The effect of forecast quantiles illustrates the sensitivity of simulated outcomes to the prescribed adjustment rule. Within a given predictive distribution, higher quantiles provide longer waiting time allowances and can lead to greater speed reductions, subject to operational constraints. This does not imply a change in the underlying predictive distribution or an operator's behavioural risk preference. In the simulated scenarios, higher quantiles generally produce larger emissions reductions, particularly when the speed-adjustment window is sufficiently long but can also increase late-arrival duration. In the upper-right areas of the response surfaces, emissions reductions begin to approach saturation while late-arrival duration continues to increase. These patterns show that allowing for longer anticipated waiting times can yield diminishing additional emissions benefits while increasing late-arrival exposure.

The response surfaces therefore provide a basis for comparing operational trade-offs across scenarios. The delay contours are descriptive references and do not establish an acceptable delay threshold. Selecting a forecast quantile and notification lead time requires consideration of berth arrangements, contractual commitments, downstream schedules and participation conditions. A scenario offering larger



Fig. 8. SHAP bee swarm plot.

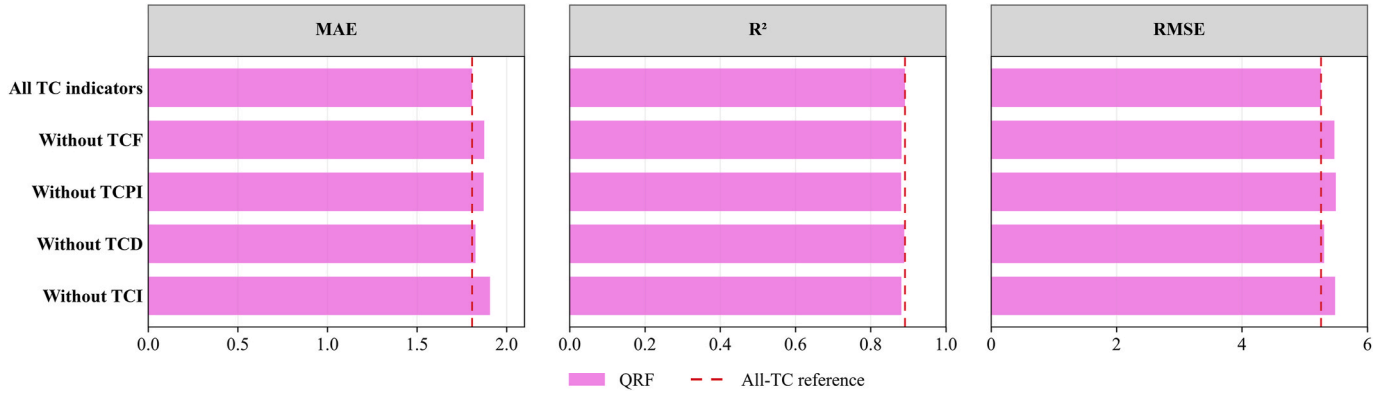

Fig. 9. QRF performance following the exclusion of individual tropical cyclone indicators.

emission reductions may be less attractive to a carrier facing tighter arrival constraints.

The middle part of the heatmaps illustrates scenarios in which emission reductions are accompanied by varying levels of late-arrival exposure. These patterns reveal trade-offs between environmental benefits and arrival delays. This finding suggests that probabilistic forecasts could support risk adjusted decisions, allowing ports and carriers to select appropriate quantile levels and coordination windows according to congestion severity, contractual schedule constraints, fuel costs and service reliability requirements.

The two port cases show broadly consistent patterns, illustrating how forecast quantiles and notification lead times shape simulated emissions and late-arrival outcomes under different operational conditions. However, the shapes of the response surfaces differ between Ningbo

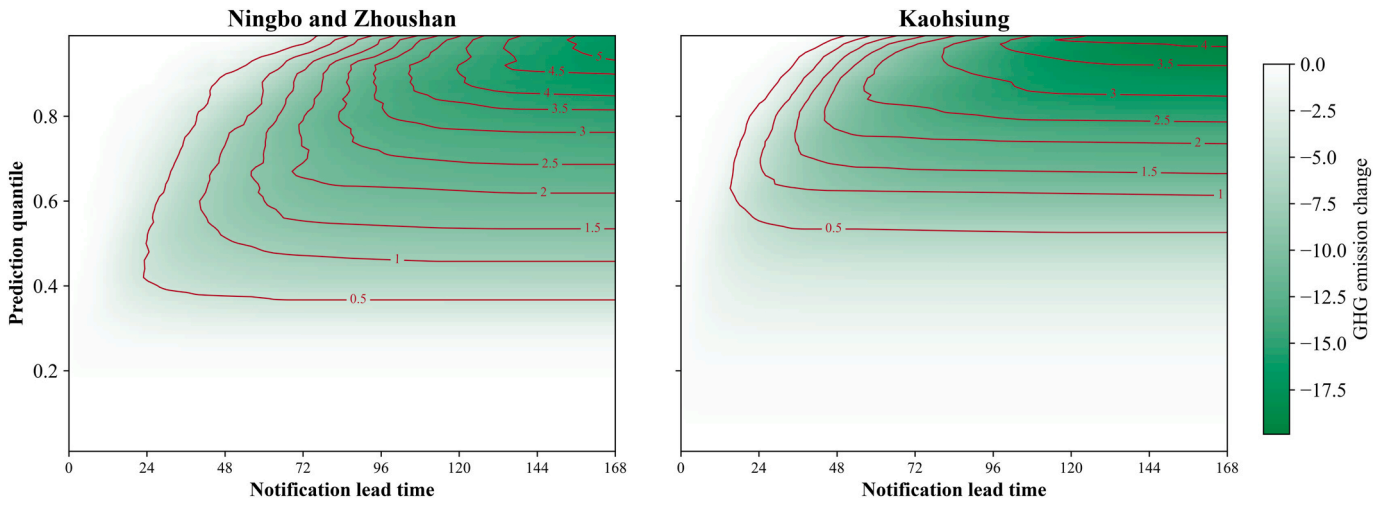

Fig. 10. GHG emission change under the speed adjustment strategy.

Zhoushan and Kaohsiung, which suggests that the effectiveness of speed adjustment depends on local recovery conditions, vessel arrival patterns and congestion intensity. This further highlights the need for port- and event-specific decision rules. From a dynamic capability's perspective, the simulations illustrate the operational options that forecast information could support within a broader coordination process. They do not directly test whether organisations successfully sense risks, agree on coordinated responses or implement operational reconfiguration. These organisational requirements are discussed in Section 5.3.

5.3. Prediction to intervention coordination process

The proposed speed-adjustment strategy informed by prediction requires coordinated action among port authorities, terminal operators and shipping companies during post-cyclone recovery. Dynamic capability theory provides an interpretative framework for explaining how these actors can translate forecast information into coordinated operational decisions. Fig. 11 illustrates the proposed sequence from risk sensing to coordinated decision-making and operational reconfiguration. Table 5 complements this process diagram by identifying the actors, decision points, information exchanges and organisational actions associated with each stage.

The sensing stage in Fig. 11 begins with the assessment of available cyclone and port information. Once the port has entered the recovery stage and the required model inputs are available, probabilistic waiting time forecasts can be generated. Port authorities and terminal operators

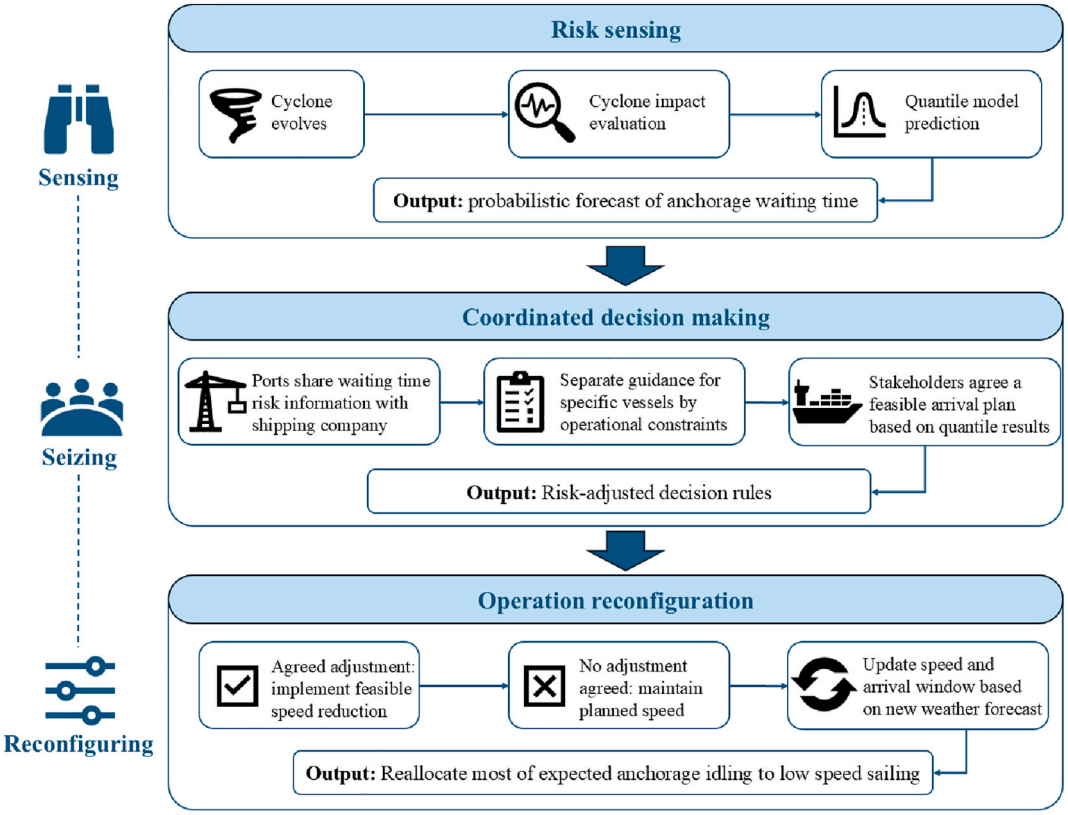

Fig. 11. Prediction to intervention coordination process for post-cyclone port recovery.

Table 5
Conceptual mapping of dynamic capabilities to forecast-informed arrival coordination.

Micro foundation	Actors	Decision point	Information exchanges	Organisational action
Sensing	Port authorities; Terminal operators; Shipping companies	When a recovery-stage forecast is issued or updated	Cyclone information; Vessel characteristics; Waiting time distributions Port activity and conditions;	Interpret waiting time risk; Identify calls requiring coordination; Communicate forecast uncertainty
Seizing	Port authorities; Terminal operators; Shipping companies	After reviewing forecasts and before agreeing on an arrival adjustment	Forecast information; Ship real time status Contract commitments; Port activity and conditions;	Agree on feasible arrival windows and adjustment plans
Reconfiguring	Port authorities; Terminal operators; Vessel masters; Shipping companies	Once an adjustment is agreed and whenever relevant conditions change	New arrival plans & ETAs; New forecast information; Ship real time status; Port activity and conditions	Implement feasible speed and arrival adjustments; Update operational plans and communicate deviations

interpret these distributions alongside current operating conditions to identify vessel calls that may require arrival coordination. Forecasting therefore provides analytical support for sensing, while the participating organisations interpret and communicate the resulting risk information.

Seizing occurs when ports, terminal operators and shipping companies evaluate the available arrival options. As illustrated in Fig. 11, ports share waiting time risk information, and guidance is differentiated according to vessel-level operational constraints. Shipping companies assess the proposed adjustments against remaining sailing distance, speed limits, downstream schedules and contractual commitments. Forecast quantiles provide alternative decision settings for this discussion, allowing the actors to agree on feasible arrival plans and the conditions under which those plans should be revised.

Reconfiguring involves implementing and updating the agreed plans. Vessels may reduce speed where forecast waiting time and operational constraints permit, while others maintain their planned speed. Shipping companies and vessel masters implement the sailing adjustments, and port and terminal operators coordinate the associated arrival arrangements. Revised ETAs, vessel progress and updated weather and port information support subsequent revisions. This stage therefore involves changes to operational plans and information exchanges, extending beyond the physical act of reducing vessel speed.

Together, Fig. 11 and Table 5 explain how forecast information could be translated into organisational action. Their implementation depends on the data-sharing responsibilities, participation incentives and risk-allocation arrangements discussed in Section 5.4. The empirical analysis evaluates predictive performance and simulated emissions and delay trade-offs under specified adjustment rules; it does not directly measure organisational capabilities or test whether stakeholders reach and implement coordinated agreements.

Forecast information does not determine vessel behaviour on its own. Operators may assign different priorities to anchorage waiting, schedule reliability, fuel savings and contractual penalties. For example, Vessel A may face a high predicted waiting time risk, but its operator may be willing to accept anchorage waiting and maintain the planned speed. Vessel B may face a low predicted waiting time risk, while its operator prioritises avoiding late arrival caused by slowing down. Under these assumed decisions, both vessels maintain their planned speeds, leaving the anticipated arrival pattern unchanged and foregoing potential arrival-smoothing and emissions-reduction benefits from speed adjustment. This does not establish that port congestion would worsen, because port-wide queueing dynamics and interactions among vessel decisions are not represented in the current simulation. Consequently, the current simulation cannot quantify how heterogeneous risk preferences would alter intervention performance. The reported emissions and late-arrival outcomes should therefore be interpreted as conditional on vessels following the prescribed speed-adjustment rules. Table 6 provides a conceptual illustration of possible responses to forecast information.

5.4. Policy implications for port recovery

Beyond the operational coordination process described above, the framework also has important implications for institutionalising forecast-informed recovery governance in ports exposed to tropical cyclones. The proposed framework implies that post-cyclone resilience should be managed through forecast-informed recovery governance rather than relying on reactive congestion control alone. In this setting, probabilistic waiting time forecasts provide an operational basis for deciding when to activate coordination protocols, which vessels should adjust their arrival profiles, and how much delay can be shifted before congestion intensifies. This approach moves resilience management beyond reopening and towards actively stabilising vessel flows, maintaining service reliability, and reducing congestion during recovery.

Effective implementation also depends on reliable data governance. Probabilistic arrival management requires timely access to vessel schedules, AIS-derived movement information, berth plans, anchorage status, terminal capacity, pilotage availability and weather forecasts (Nguyen et al., 2026). These data are often distributed across port authorities, terminal operators, shipping companies, vessel traffic services

Table 6
Illustrative interactions between predicted waiting time risk and vessel decision preferences.

Predicted waiting time risk	Decision preferences	Implications for arrival coordination	Potential Results
Low for both vessels	Both prioritise schedule target; Limited schedule flexibility	Limited scope for arrival adjustment	Limited emissions savings
High for both vessels	Both accept arrival adjustment Sufficient schedule flexibility	Joint adjustment requiring coordination	Potential savings for both; Late-arrival risk
High for both vessels	Vessel A accepts adjustment; Vessel B prioritise schedule target	Selective adjustment affecting arrival spacing	Potential savings for A; Possible anchorage waiting for B
High for both vessels	Both prioritise arrival schedule target	No adjustment to anticipated arrival clustering	No adjustment-related savings; Possible anchorage waiting for both
High for A and low for B	Both accept arrival adjustment	Selective adjustment based on vessel-specific risk	Potential savings for A; Late-arrival risk
High for A and low for B	Vessel A accepts anchorage waiting and maintains speed; Vessel B prioritise schedule target	Both maintain their planned speeds; the anticipated arrival pattern remains unchanged.	No emissions savings; Remains exposed to prolonged anchorage waiting.

Notes: These scenarios provide a conceptual illustration of possible stakeholder responses.

and meteorological agencies. A port community system or regional maritime data platform is therefore needed to integrate fragmented information sources and support shared situational awareness (Nikghadam et al., 2023). Beyond technical integration, clear rules are needed for data ownership, update frequency, data quality standards and responsibility for forecast dissemination. Without trusted data sharing mechanisms, even accurate prediction models may have only a limited influence on operational decisions.

Shifting part of the expected anchorage waiting time into controlled low speed sailing can reduce fuel consumption and GHG emissions, but it may also create a risk of late arrival if the realised waiting time is shorter than predicted. This risk is not borne equally by all actors. Carriers may face contractual penalties, service schedule disruption or reduced buffer time, while ports and terminals may benefit from smoother arrival flows and lower anchorage congestion (Li et al., 2016; Mulder and Dekker, 2019). Practical implementation therefore requires mechanisms for sharing the costs and benefits of arrival adjustment informed by forecasts. Flexible berth windows during tropical cyclone recovery, temporary relaxation of arrival punctuality penalties, sharing of fuel-saving benefits and port fee incentives for vessels that follow coordinated recovery guidance could all help improve stakeholder acceptance. These mechanisms are proposed conditions for supporting participation; their effectiveness is not evaluated in the present simulation. The simulated outcomes remain conditional on vessels following the specified speed adjustment rules.

Post-cyclone coordination can also complement port decarbonisation strategies. Many port emission reduction measures focus on infrastructure investment, alternative fuels, shore power or equipment electrification (Sun et al., 2025b). These measures are important, but they often require long planning cycles and substantial capital investment. By contrast, speed adjustment based on forecast information is a short-term operational measure that can be implemented through existing vessel and port coordination systems (Nguyen et al., 2026). This is particularly important during recovery, when anchorage queues may sharply increase auxiliary engine use. Incorporating probabilistic congestion forecasts into green port policies would allow ports to address not only emissions under normal operating conditions, but also emission peaks caused by disruptions.

Regional recovery after tropical cyclones should also be considered. Tropical cyclones often affect multiple ports within the same coastal region, and recovery measures at one port may influence vessel arrival patterns at neighbouring ports (Wang et al., 2026; Xu et al., 2024). If vessels independently adjust timetable, congestion may be displaced rather than reduced. Regional maritime authorities and port clusters could therefore use shared probabilistic forecasting systems to coordinate arrival flows across ports during major cyclone events. This is particularly relevant in dense port regions such as East Asia, where major ports are closely connected through liner networks and feeder services (Jian et al., 2019; Noorali et al., 2022). Regional coordination can help prevent isolated port level optimisation from creating spillover effects elsewhere in the maritime network.

Overall, the value of this framework lies in helping ports and carriers determine when speed adjustment is beneficial, under what level of risk it remains acceptable, and how trade-offs among emissions, delay and service reliability can be managed transparently. By linking probabilistic sensing with institutional protocols, data governance, incentive mechanisms and regional coordination, the framework provides a practical pathway towards more resilient port recovery.

These arrangements should also specify who is responsible for issuing and updating forecasts, confirming arrival adjustments and communicating deviations. Port authorities can coordinate information exchange, terminal operators can confirm operational readiness, and shipping companies can communicate the feasibility and implementation of vessel-level adjustments. Clear responsibilities are necessary to translate shared forecasts into coordinated action.

6. Conclusions

This study investigates congestion dynamics during the recovery phase following tropical cyclone disruptions and proposes a prediction to intervention framework that links probabilistic waiting time forecasting with risk-aware operational intervention. By focusing on vessel waiting time as a direct indicator of port efficiency loss, the analysis shows how extreme weather shocks can propagate through port systems and generate downstream congestion after port reopening. In doing so, the study extends the assessment of port resilience from whether operations resume to how quickly port efficiency, vessel flows, and schedule reliability recover to an acceptable level.

The empirical results show that training on cyclone-related observations substantially improves the predictive performance of QRF and RF compared with training under normal operating conditions. Adding cyclone-port indicators provides a further improvement in QRF's point prediction accuracy, with an MAE of 1.808 h, an RMSE of 5.260 h and an R^2 of 0.891. QRF performs best among the evaluated models under this setting. SHAP analysis highlights the predictive importance of port traffic composition, short-term demand and facility characteristics, while the ablation experiments support the incremental contribution of the four cyclone indicators to point prediction. Distributional forecasts provide waiting time ranges and category probabilities, allowing stakeholders to assess waiting time risk more explicitly. Their calibration nevertheless requires further attention, as the reported prediction intervals exhibit coverage above the nominal level.

The study further demonstrates how predictive information can be translated into speed-adjustment scenarios. Scenario analysis indicates that forecast quantiles and notification lead times jointly shape the trade-off between emissions reduction and late-arrival exposure. In the two illustrative port cases, shifting part of the anchorage waiting time into controlled low-speed sailing reduces simulated emissions across much of the scenario range. Higher forecast quantiles and longer notification lead times can produce additional savings, although these benefits may level off as late-arrival exposure increases. The analysis supports scenario comparison without establishing a universally acceptable delay threshold or an optimal operating rule.

From a theoretical perspective, the findings illustrate how predictive analytics can support dynamic capabilities in disruption-prone maritime environments. Distributional forecasting enables ports and shipping actors to transform uncertain cyclone-port signals into comparable risk measures for coordination. The conceptual mapping identifies how port authorities and terminal operators can interpret forecasts to support sensing, how ports and carriers can agree on feasible arrival adjustments through seizing, and how participating organisations can implement and update operational plans through reconfiguring. This provides an organisational interpretation of the framework; the capabilities themselves are not directly measured or tested.

From a policy and managerial perspective, the study shows that post-cyclone recovery should be treated not only as an operational forecasting problem, but also as a governance challenge involving data sharing, risk allocation and inter-organisational coordination. Embedding probabilistic forecasts into formal recovery protocols, port community systems and regional coordination mechanisms could support more coordinated arrival management. Implementation requires clear responsibilities for forecast updates and arrival agreements, alongside arrangements that address the contractual constraints and participation incentives of shipping companies.

Several limitations remain. The East Asian focus and two intervention cases provide limited evidence of transferability to other ports and fleets. The framework predicts waiting time distributions rather than congestion occurrence. Future research could first estimate congestion probability and then predict waiting times conditional on congestion. The simulation also assumes compliance and excludes heterogeneous carrier preferences and strategic interactions, and therefore cannot quantify their effects on intervention performance. Forecast quantiles

determine waiting time allowances within the adjustment rule rather than represent behavioural risk preferences. Future research could integrate behavioural choice models with agent-based or game-theoretic approaches to examine how heterogeneous preferences and interacting vessel decisions affect port-wide congestion and intervention effectiveness.

CRediT authorship contribution statement

Ruikai Sun: Writing – original draft, Software, Methodology, Investigation, Formal analysis, Data curation, Conceptualization, Resources, Validation, Visualization, Writing – review & editing. **Huanhuan Li:** Writing – review & editing, Validation, Supervision, Methodology, Conceptualization, Investigation, Project administration, Resources, Visualization. **Hao Rong:** Writing – review & editing, Visualization, Supervision, Investigation, Methodology, Validation, Project administration, Formal analysis. **Zaili Yang:** Writing – review & editing, Supervision, Funding acquisition, Conceptualization, Project administration, Resources.

Acknowledgement

This project has received funding from the European Research Council (ERC) under the European Union's Horizon 2020 research and innovation programme (Grant Agreement No. 864724)

Appendix A. Sensitivity analysis using an expanded event sample

The expanded-sample analysis includes 19 additional cyclone-port events without observed post-cyclone congestion, bringing the total to 76 events and 6996 distinct vessel calls, while maintaining the same experimental settings as the main analysis. As shown in Fig. A.1, QRF remains the best-performing model among the ten models, achieving the lowest MAE and RMSE and the highest R^2.

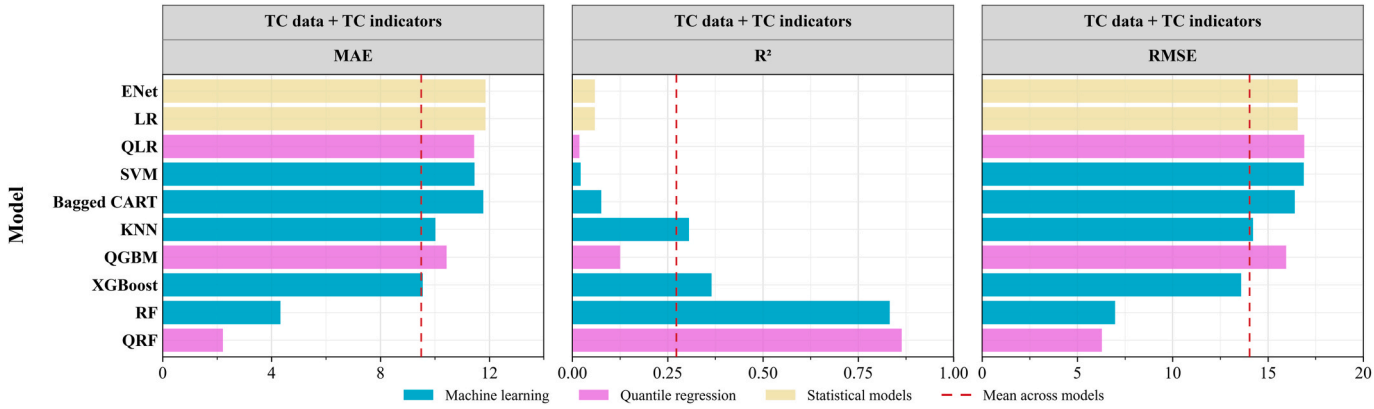

Fig. A.1. Model performance on expanded sample.

Appendix B. Model training setting

Table B.1
Data splitting results

Data set	Data type	Event number	Port call
Benchmark	Training data	47	6692
TC data		47	2207
TC data + TC indicators		47	2207
TC data + BWT		47	2207
TC data + TC indicators + BWT		47	2207
All test data	Test data	8	389

Table B.2
Number of retained predictors and selected LASSO penalty parameters across modelling settings.

Modelling setting	Code	Number of retained predictors	Selected penalty parameter (λ)
Benchmark	S1	16	5.90×10^{-5}
TC data	S2	16	3.10×10^{-5}
TC data + TC indicators	S3	20	7.17×10^{-5}
TC data + BWT	S4	17	3.41×10^{-5}
TC data + TC indicators + BWT	S5	21	9.49×10^{-5}

Table B.3
LASSO coefficient across modelling settings.

Predictor	S1	S2	S3	S4	S5
DWT	−2.78E-02	5.13E-02	3.59E-02	4.99E-02	3.63E-02
DRA	2.60E-01	1.78E-01	1.89E-01	1.87E-01	1.89E-01
LOA	1.73E-01	−1.07E-01	−7.07E-02	−8.03E-02	−7.07E-02
BEAM	−2.60E-01	−1.05E-01	−1.18E-01	−1.54E-01	−1.20E-01
Built	9.53E-04	1.08E-03	9.86E-04	1.36E-03	1.00E-03
SSP	−4.66E-04	5.14E-03	4.74E-03	3.79E-03	4.61E-03
MER	7.15E-03	−6.39E-02	−6.26E-02	−6.41E-02	−6.19E-02
MEP	−3.11E-02	−5.61E-02	−5.76E-02	−5.31E-02	−5.67E-02
BulkP	−1.41E-01	−2.17E-01	−2.26E-01	−1.88E-01	−2.20E-01
ContP	−6.30E-02	2.38E-01	6.06E-02	2.79E-01	6.59E-02
CityP	−1.49E-08	−1.35E-08	−1.34E-08	−1.38E-08	−1.34E-08
FCAP	−3.76E-03	−4.40E-03	8.13E-04	−4.31E-03	7.73E-04
ANDWT	1.26E-09	1.06E-09	1.06E-09	1.07E-09	1.06E-09
PDWT	7.97E-02	1.11E-01	1.00E-01	1.02E-01	9.99E-02
PNUM	6.14E-02	−6.82E-02	−4.38E-02	−5.23E-02	−4.29E-02
MAXD	−1.27E-03	8.38E-03	−1.22E-02	7.53E-03	−1.17E-02
TCF	N/A	N/A	−7.51E-03	N/A	−7.57E-03
TCPI	N/A	N/A	−3.41E-01	N/A	−3.39E-01
TCD	N/A	N/A	−1.56E-03	N/A	−1.57E-03
TCI	N/A	N/A	1.27E-03	N/A	1.26E-03
BWT	N/A	N/A	N/A	−2.29E-01	−2.40E-02
Intercept	−1.70E+00	−1.34E+00	−5.59E-01	−1.87E+00	−6.06E-01

Data availability

The authors do not have permission to share data.

References

Abdelhafez, A.M., Ellingwood, B., Mahmoud, H., 2021. Vulnerability of seaports to hurricanes and sea level rise in a changing climate: a case study for mobile, AL. Coast. Eng. 167, 103884. https://doi.org/10.1016/j.coastaleng.2021.103884.

Alessandrini, A., Mazzarella, F., Vespe, M., 2019. Estimated time of arrival using historical vessel tracking data. IEEE Trans. Intell. Transport. Syst. 20 (1), 7–15. https://doi.org/10.1109/TITS.2017.2789279.

Arora, S., Taylor, J.W., Mak, H.-Y., 2023. Probabilistic forecasting of patient waiting times in an emergency department. Manuf. Serv. Oper. Manag. 25 (4), 1489–1508. https://doi.org/10.1287/msom.2023.1210.

Balci, G., Balci, E.S., Iris, Ç., 2026. The role of human capital and Industry 4.0 in socio-technical dynamic capabilities for freight transport resilience. Transp. Res. A: Policy Pract. 204, 104784.

Bathke, H., Münch, C., von der Gracht, H.A., Hartmann, E., 2024. Building resilience through foresight: the case of maritime container shipping firms. IEEE Trans. Eng. Manag. 71, 10534–10556. https://doi.org/10.1109/TEM.2021.3137009.

Bruneau, M., Chang, S.E., Eguchi, R.T., Lee, G.C., O'Rourke, T.D., Reinhorn, A.M., Shinozuka, M., Tierney, K., Wallace, W.A., von Winterfeldt, D., 2003. A framework to quantitatively assess and enhance the seismic resilience of communities. Earthq. Spectra 19 (4), 733–752. https://doi.org/10.1193/1.1623497.

Cao, X., Lam, J.S.L., 2018. Simulation-based catastrophe-induced port loss estimation. Reliab. Eng. Syst. Saf. 175, 1–12. https://doi.org/10.1016/j.ress.2018.02.008.

Chambers, J.M., Hastie, T.J., 1992. Statistical models. In: Statistical Models in S. Routledge.

Chen, W., Chen, J., Geng, J., Ye, J., Yan, T., Shi, J., Xu, J., 2023. Monitoring and evaluation of ship operation congestion status at container ports based on AIS data. Ocean Coast Manag. 245, 106836. https://doi.org/10.1016/j.ocecoaman.2023.106836.

Choi, M.-H., Yoon, W., 2025. Predicting ship waiting times using machine learning for enhanced port operations. IEEE Access 13, 81377–81391. https://doi.org/10.1109/ACCESS.2025.3566429.

Chu, Z., Yan, R., Wang, S., 2024. Evaluation and prediction of punctuality of vessel arrival at port: a case study of Hong Kong. Marit. Pol. Manag. 51 (6), 1096–1124. https://doi.org/10.1080/03088839.2023.2217168.

Dovbischuk, I., 2022. Innovation-oriented dynamic capabilities of logistics service providers, dynamic resilience and firm performance during the COVID-19 pandemic. Int. J. Logist. Manag. 33 (2), 499–519. https://doi.org/10.1108/IJLM-01-2021-0059.

Gong, J., Li, H., Jiao, H., Yang, Z., 2025. Uncertainty-aware ship trajectory prediction via Spatio-Temporal Graph Transformer. Transport. Res. E Logist. Transport. Rev. 203, 104315. https://doi.org/10.1016/j.tre.2025.104315.

Hall, P., 1992. Effect of bias estimation on coverage accuracy of bootstrap confidence intervals for a probability density. Ann. Stat. 20 (2), 675–694.

Hersbach, H., 2000. Decomposition of the continuous ranked probability Score for ensemble prediction systems. Weather Forecast. 15 (5), 559–570. https://doi.org/10.1175/1520-0434(2000)015%3C0559:DOTCRP%3E2.0.CO;2.

Huang, Z., He, Z., Zhao, P., Zhang, C., Niu, Y., Guo, W., Cui, Y., Shao, W., 2024. The effects of tropical cyclone on the container shipping network: a case study of typhoon Ma-on (2022). Transport. Res. Transport Environ. 136, 104449. https://doi.org/10.1016/j.trd.2024.104449.

Huang, Z., Wang, D., Yin, Y., Cheng, T.C.E., 2025. A prediction interval framework-based spatial–temporal convolution block network for traffic demand prediction. Transport. Res. E Logist. Transport. Rev. 204, 104426. https://doi.org/10.1016/j.tre.2025.104426.

IMO, 2020a. Fourth IMO Greenhouse Gas Study 2020. International Maritime Organization. https://greenvoyage2050.imo.org/wp-content/uploads/2021/07/Fourth-IMO-GHG-Study-2020-Full-report-and-annexes_compressed.pdf.

IMO, 2020b. Fourth IMO Greenhouse Gas Study 2020. International Maritime Organization.

Izaguirre, C., Losada, I.J., Camus, P., Vigh, J.L., Stenek, V., 2021. Climate change risk to global port operations. Nat. Clim. Change 11 (1), 14–20. https://doi.org/10.1038/s41558-020-00937-z.

Jian, W., Liu, C., Lam, J.S.L., 2019. Cyclone risk model and assessment for East Asian container ports. Ocean Coast Manag. 178, 104796. https://doi.org/10.1016/j.ocecoaman.2019.04.023.

Jiang, S., Liu, L., Peng, P., Xu, M., Yan, R., 2024. Prediction of vessel arrival time to port: a review of current studies. Marit. Pol. Manag. 0 (0), 1–26. https://doi.org/10.1080/03088839.2025.2488376.

Jo, A.-H., Chang, Y.-T., Lee, H., Cho, S.-H., 2025. Estimating vessel waiting time using queuing models. Marit. Econ. Logist. https://doi.org/10.1057/s41278-025-00319-2.

Kang, L., Hansen, M., 2021. Quantile regression–based estimation of dynamic statistical contingency fuel. Transp. Sci. 55 (1), 257–273. https://doi.org/10.1287/trsc.2020.0997.

Kong, X., Wang, K., Hou, M., Xia, F., Karmakar, G., Li, J., 2022. Exploring human mobility for multi-pattern passenger prediction: a graph learning framework. IEEE Trans. Intell. Transport. Syst. 23 (9), 16148–16160. https://doi.org/10.1109/TITS.2022.3148116.

Kuo, S.-Y., Lin, P.-C., Lu, C.-S., 2017. The effects of dynamic capabilities, service capabilities, competitive advantage, and organizational performance in container shipping. Transport. Res. Pol. Pract. 95, 356–371. https://doi.org/10.1016/j.tra.2016.11.015.

Lam, J.S.L., Liu, C., Gou, X., 2017. Cyclone risk mapping for critical coastal infrastructure: cases of East Asian seaports. Ocean Coast Manag. 141, 43–54. https://doi.org/10.1016/j.ocecoaman.2017.02.015.

Li, C., Qi, X., Song, D., 2016. Real-time schedule recovery in liner shipping service with regular uncertainties and disruption events. Transp. Res. Part B: Methodological, Maritime Logistics 93, 762–788. https://doi.org/10.1016/j.trb.2015.10.004.

Li, X., Chua, J.Y., Yuen, K.F., 2024. A review on maritime disruption management: categories, impacts, and strategies. Transp. Policy 154, 40–47. https://doi.org/10.1016/j.tranpol.2024.05.013.

Liu, K.S., Chan, J.C.L., 2022. Growing threat of rapidly-intensifying tropical cyclones in east Asia. Adv. Atmos. Sci. 39 (2), 222–234. https://doi.org/10.1007/s00376-021-1126-7.

Liu, M., Lai, K., Liu, Y., Wong, C.W.Y., Chen, J., Yang, Z., 2026. Make waves: quantifying the impact of the Red Sea crisis on global container port turnaround time. Transport. Res. E Logist. Transport. Rev. 214, 105050. https://doi.org/10.1016/j.tre.2026.105050.

Liu, Y., Fu, X., Wang, K., Zheng, S., Xiao, Y., 2025. Bibliometric analysis and literature review on maritime transport resilience and its associated impacts on trade. Marit. Pol. Manag. 52 (3), 440–477. https://doi.org/10.1080/03088839.2024.2367971.

Mattsson, L.-G., Jenelius, E., 2015. Vulnerability and resilience of transport systems – a discussion of recent research. Transp. Res. Part A: Policy and Practice, Resilience of Networks 81, 16–34. https://doi.org/10.1016/j.tra.2015.06.002.

Mikalef, P., Boura, M., Lekakos, G., Krogstie, J., 2019. Big data analytics capabilities and innovation: the mediating role of dynamic capabilities and moderating effect of the environment. Br. J. Manag. 30 (2), 272–298. https://doi.org/10.1111/1467-8551.12343.

Mohsendokht, M., Kontovas, C., Chang, C.-H., Qu, Z., Li, H., Yang, Z., 2026a. Resilience analysis of seaports: a critical review of development and research directions. Marit. Pol. Manag. 53 (2), 227–262. https://doi.org/10.1080/03088839.2025.2483410.

Mohsendokht, M., Mokhtari-Moghadam, A., Li, H., Kontovas, C., Chang, C.-H., Qu, Z., Yang, Z., 2026b. A risk-based simulation approach to assessing seaport resilience against cyclone hazards. Transport. Res. Transport Environ. 154, 105291. https://doi.org/10.1016/j.trd.2026.105291.

Mulder, J., Dekker, R., 2019. Designing robust liner shipping schedules: optimizing recovery actions and buffer times. Eur. J. Oper. Res. 272 (1), 132–146. https://doi.org/10.1016/j.ejor.2018.05.066.

Muthukrishnan, R., Rohini, R., 2016. LASSO: a feature selection technique in predictive modeling for machine learning. 2016 IEEE International Conference on Advances in Computer Applications (ICACA), pp. 18–20. https://doi.org/10.1109/ICACA.2016.7887916.

Neise, T., Revilla Diez, J., 2019. Adapt, move or surrender? Manufacturing firms' routines and dynamic capabilities on flood risk reduction in coastal cities of Indonesia. Int. J. Disaster Risk Reduct. 33, 332–342. https://doi.org/10.1016/j.ijdrr.2018.10.018.

Nguyen, S., Fu, X., Zhao, L., Xu, H., Zhang, X., Li, N., Zhang, W., Yin, X.F., Daichi, O., Koh, J., Zheng, Q., 2026. AI-driven just-in-time coordination between port and ships: advancing maritime decarbonization. Transport. Res. E Logist. Transport. Rev. 207, 104569. https://doi.org/10.1016/j.tre.2025.104569.

Nikghadam, S., Molkenboer, K.F., Tavasszy, L., Rezaei, J., 2023. Information sharing to mitigate delays in port: the case of the Port of Rotterdam. Marit. Econ. Logist. 25 (3), 576–601. https://doi.org/10.1057/s41278-021-00203-9.

Noorali, H., Flint, C., Ahmadi, S.A., 2022. Port power: towards a new geopolitical world order. J. Transport Geogr. 105, 103483. https://doi.org/10.1016/j.jtrangeo.2022.103483.

Prayag, G., Jiang, Y., Chowdhury, M., Hossain, M.I., Akter, N., 2024. Building dynamic capabilities and organizational resilience in tourism firms during COVID-19: a staged approach. J. Trav. Res. 63 (3), 713–740. https://doi.org/10.1177/00472875231164976.

Qin, Y., Guo, J., Wu, S., 2025. The resilience evolution and dynamic process identification of the global shipping network. Transp. Policy 174, 103851. https://doi.org/10.1016/j.tranpol.2025.103851.

Saber, S. Md, Thowai, K.Z., Rahman, M.A., Hassan, Md M., Bari, A.B.M.M., Raihan, A., 2025. High-accuracy prediction of vessels' estimated time of arrival in seaports: a hybrid machine learning approach. Maritime Transport Research 8, 100133. https://doi.org/10.1016/j.martra.2025.100133.

Stadtfeld, G.M., Gruchmann, T., 2023. Dynamic capabilities for supply chain resilience: a meta-review. Int. J. Logist. Manag. 35 (2), 623–648. https://doi.org/10.1108/IJLM-09-2022-0373.

Stott, P., 2016. How climate change affects extreme weather events. Science 352 (6293), 1517–1518. https://doi.org/10.1126/science.aaf7271.

Sun, R., Abouarghoub, W., Demir, E., 2025a. Enhancing data quality in maritime transportation: a practical method for imputing missing ship static data. Ocean. Eng. 315, 119722.

Sun, R., Abouarghoub, W., Demir, E., Potter, A., 2025b. A comprehensive analysis of strategies for reducing GHG emissions in maritime ports. Mar. Pol. 171, 106455. https://doi.org/10.1016/j.marpol.2024.106455.

Tak, S., Kim, S., Oh, S., Yeo, H., 2016. Development of a data-driven framework for real-time travel time prediction. Comput. Aided Civ. Infrastruct. Eng. 31 (10), 777–793. https://doi.org/10.1111/mice.12205.

Teece, D.J., 2007. Explicating dynamic capabilities: the nature and microfoundations of (sustainable) enterprise performance. Strateg. Manag. J. 28 (13), 1319–1350. https://doi.org/10.1002/smj.640.

Teece, D.J., Pisano, G., Shuen, A., 1997. Dynamic capabilities and strategic management. Strateg. Manag. J. 18 (7), 509–533. https://doi.org/10.1002/(SICI)1097-0266(199708)18:7%3C509::AID-SMJ882%3E3.0.CO;2-Z.

Tibshirani, R., 1996. Regression shrinkage and selection via the lasso. J. Roy. Stat. Soc. B Stat. Methodol. 58 (1), 267–288.

Uyanık, T., Karatuğ, Ç., Arslanoğlu, Y., 2020. Machine learning approach to ship fuel consumption: a case of container vessel. Transport. Res. Transport Environ. 84, 102389. https://doi.org/10.1016/j.trd.2020.102389.

Veenstra, A., Harmelink, R., 2021. On the quality of ship arrival predictions. Marit. Econ. Logist. 23 (4), 655–673. https://doi.org/10.1057/s41278-021-00187-6.

Verschuur, J., Koks, E.E., Hall, J.W., 2020. Port disruptions due to natural disasters: insights into port and logistics resilience. Transport. Res. Transport Environ. 85, 102393. https://doi.org/10.1016/j.trd.2020.102393.

Wan, C., Yang, Z., Zhang, D., Yan, X., Fan, S., 2018. Resilience in transportation systems: a systematic review and future directions. Transp. Rev. 38 (4), 479–498. https://doi.org/10.1080/01441647.2017.1383532.

Wang, H.-W., Peng, Z.-R., Wang, D., Meng, Y., Wu, T., Sun, W., Lu, Q.-C., 2020. Evaluation and prediction of transportation resilience under extreme weather events: a diffusion graph convolutional approach. Transport. Res. C Emerg. Technol. 115, 102619. https://doi.org/10.1016/j.trc.2020.102619.

Wang, T., Feng, H., Poo, M.C.-P., Lau, Y.-Y., 2024a. Analysis of the network efficiency of Chinese ports in global shipping under the impacts of typhoons. Sustainability 16 (8). https://doi.org/10.3390/su16083190.

Wang, T., Ng, A.K.Y., Wang, J., Chen, Q., Pang, J., Tang, J., 2024b. Adaptation planning of container ports in the context of typhoon risks: the case of Ningbo-Zhoushan port in China. Ocean Coast Manag. 257, 107303. https://doi.org/10.1016/j.ocecoaman.2024.107303.

Wang, T., Xu, T.Z., Feng, H., Guo, Z., Poo, M.C.-P., Tang, J., Ng, A.K.Y., 2026. Enhancing port resilience to typhoon disasters: a framework for recovery optimization and shipping network impact assessment. Transp. Policy 180, 104029. https://doi.org/10.1016/j.tranpol.2026.104029.

Winter, S.G., 2003. Understanding dynamic capabilities. Strateg. Manag. J. 24 (10), 991–995. https://doi.org/10.1002/smj.318.

Wohlleber, A.J., Bock, M., Birkel, H., Hartmann, E., 2024. Implementing vital dynamic capabilities to succeed in digital transformation: a multiple-case Study in maritime container shipping. IEEE Trans. Eng. Manag. 71, 13627–13645. https://doi.org/10.1109/TEM.2022.3201770.

Xu, L., Hou, Z., Song, Y., Chen, J., Shu, Y., 2026. A feature selection-enhanced machine learning framework for clean-energy shipbuilding predictions. Ocean Coast Manag. 276, 108175. https://doi.org/10.1016/j.ocecoaman.2026.108175.

Xu, M., Zhu, Y., Liu, K., Ng, A.K.Y., 2024. Assessing resilience of global liner shipping network to tropical cyclones. Transport. Res. Transport Environ. 131, 104189. https://doi.org/10.1016/j.trd.2024.104189.

Yan, Z., Yang, G., He, R., Shi, K., Yang, H., 2025. Reconstructing trajectories and extracting shipping routes between ports based on AIS data. Appl. Ocean Res. 161, 104709. https://doi.org/10.1016/j.apor.2025.104709.

Yang, C.-C., Hsu, W.-L., 2018. Evaluating the impact of security management practices on resilience capability in maritime firms—A relational perspective. Transport. Res. Pol. Pract. 110, 220–233. https://doi.org/10.1016/j.tra.2017.06.005.

Yang, C.-S., 2026. Geopolitical disruptions and sustainability imperatives: a structural model of value chain and supply chain transformation in maritime logistics. Transport. Res. E Logist. Transport. Rev. 209, 104733. https://doi.org/10.1016/j.tre.2026.104733.

Yoon, J.-H., Kim, D.-H., Yun, S.-W., Kim, H.-J., Kim, S., 2023. Enhancing container vessel arrival time prediction through past voyage route modeling: a case Study of Busan new port. J. Mar. Sci. Eng. 11 (6), 1234. https://doi.org/10.3390/jmse11061234.

Yu, J., Tang, G., Song, X., Yu, X., Qi, Y., Li, D., Zhang, Y., 2018. Ship arrival prediction and its value on daily container terminal operation. Ocean. Eng. 157, 73–86. https://doi.org/10.1016/j.oceaneng.2018.03.038.

Zhang, C., Zhao, P., Huang, Z., He, Z., Niu, Y., Huang, G., Chen, Y., 2024. Assessing vessel transportation delays affected by tropical cyclones using AIS data and a bayesian network: a case study of veronica in northwestern Australia. Ocean. Eng. 308, 118385. https://doi.org/10.1016/j.oceaneng.2024.118385.

Zhang, H., Guo, J., Guo, S., 2025. An optimization study on dynamic berth allocation based on vessel arrival time prediction. Ocean. Eng. 332, 121321. https://doi.org/10.1016/j.oceaneng.2025.121321.

Zhou, Z.-H., 2021. Machine Learning. Springer Nature.